

issn 0065-3713

INSTITUT D'AÉRONOMIE SPATIALE DE BELGIQUE

3 - Avenue Circulaire

B - 1180 BRUXELLES

## AERONOMICA ACTA

A - N° 322 - 1987

The potential impact on atmospheric ozone and  
temperature of increasing trace gas concentrations

by

G. BRASSEUR and A. DE RUDDER

BELGISCH INSTITUUT VOOR RUIMTE-AERONOMIE

3 - Ringlaan

B - 1180 BRUSSEL

## FOREWORD

This text constitutes a report written at the request of the Commission of the European Communities (DG XI). A reduced version of this document will be published in the Journal of Geophysical Research.

## AVANT-PROPOS

Cette note constitue un rapport rédigé à la demande de la Commission des Communautés Européennes (DG XI). Une version raccourcie de ce document sera publiée dans le Journal of Geophysical Research.

## VOORWOORD

Deze tekst vormt een rapport opgesteld op verzoek van de Commissie van de Europese Gemeenschappen (DG XI). Een beknopte versie van dit document zal in het Journal of Geophysical Research gepubliceerd worden.

## VORWORT

Dieser Text enthält ein Bericht aufgesetzt auf Bitte der Kommission der Europäischen Gemeinschaften (DG XI). Eine gekürzte Ausgabe dieses Dokumentes wird in den Journal of Geophysical Research publiziert werden.

THE POTENTIAL IMPACT ON ATMOSPHERIC OZONE AND TEMPERATURE OF INCREASING  
TRACE GAS CONCENTRATIONS

by

G. BRASSEUR and A. DE RUDDER

Abstract

The response of the atmosphere to emissions of chlorofluorocarbons (CFCs) and other chlorocarbons (ClCs), and to increasing concentrations of other radiatively active trace gases such as  $\text{CO}_2$ ,  $\text{CH}_4$  and  $\text{N}_2\text{O}$  is calculated by means of a coupled chemical-radiative-transport one-dimensional model. It is shown that significant reductions in the ozone concentration and in the temperature should be expected in the upper stratosphere as a result essentially of increasing concentrations of active chlorine produced by photodecomposition of the CFCs. For a constant emission of chlorofluorocarbons -11 and -12 at approximately the 1980 level (309 kT/yr for F-11 and 433 kT/yr for F-12), the calculated decrease (assuming no other changes) in the ozone concentration relative to the preindustrial atmosphere is approximately 60-70% at 40 km and the reduction in the ozone column is 8.7% when temperature feedback is included in the model and 5.5% when it is omitted. The model also shows that a doubling of  $\text{CO}_2$  leads to a 1.8% increase in the ozone column abundance and a 2 K increase in the surface temperature. At 40 km, the ozone density is enhanced by 15% and the temperature reduced by 8 K. A doubling of methane produces a 2.4% increase in the ozone column. A 20% enhancement in the nitrous oxide content leads to an ozone depletion of 1.4%.

Time-dependent calculations of ozone and temperature show that if the production of F-11 and F-12 increases by 3%/yr. until it reaches a capacity cap equal to 1.5 times the 1985 world production level, the maximum ozone depletion should be of the order of 4 to 5%, assuming a growth in the concentration of  $\text{CO}_2$ ,  $\text{CH}_4$  and  $\text{N}_2\text{O}$  of about 0.5, 1.0 and 0.25%/yr respectively. For this scenario, the maximum ozone depletion is found to occur in year 2070. The slight increase appearing after 2070 is directly dependent on the future growth in the methane concentration.

If the production of F-11 and F-12 increases continuously by 3%/yr., without capacity cap, and if the changes in the concentration of other trace gases are ignored, the ozone column abundance is predicted to be reduced by more than 10% after year 2050.

The model shows an almost linear relation between the ozone depletion and the chlorine content as long as the mixing ratio of active chlorine remains smaller than that of active nitrogen. The  $\text{O}_3/\text{Cl}_x$  sensitivity however is a strong function of the  $\text{NO}_y$  content. For amounts of chlorine comparable or larger than those of active nitrogen, the ozone depletion increases rapidly with the amount of chlorine present in the atmosphere.

## Résumé

Un modèle à une dimension, combinant réactions chimiques, processus radiatifs et transport vertical, sert à calculer la réponse de l'atmosphère à des émissions de chlorofluorocarbones (CFCs), d'autres chlorocarbones (ClCs) et à l'augmentation de la concentration d'autres gaz sources radiativement actifs tels que  $\text{CO}_2$ ,  $\text{CH}_4$  et  $\text{N}_2\text{O}$ . Il apparaît que, dans la haute stratosphère, l'on doit s'attendre à d'appréciables diminutions de la température et de la concentration d'ozone dues principalement à l'augmentation du nombre d'atomes de chlore issu de la photolyse des CFCs. Dans le cas d'une émission constante des chlorofluorocarbones -11 et -12 valant à peu près celle de 1980 (309 kT/an pour F-11 et 433 kT/an pour F-12) et par rapport à sa valeur dans l'atmosphère préindustrielle, la concentration d'ozone diminue de 60 à 70% environ à 40 km. La diminution correspondante du contenu atmosphérique total (colonne) du même gaz est de 8,7% lorsque la rétroaction de la température sur la chimie est incluse dans le modèle, et de 5,5% quand elle ne l'est pas. Le doublement de la concentration en  $\text{CO}_2$  conduit quant à lui à une augmentation de 1,8% de la colonne d'ozone et à une hausse de la température de surface de 2 K. A 40 km, la concentration d'ozone s'accroît dans ce cas de 15% et la température diminue de 8 K. La colonne d'ozone augmente de 2,4% si l'on double la concentration en méthane; elle diminue de 1,4% pour une augmentation de 20% en hémioxyde d'azote.

Le calcul de la quantité totale d'ozone en fonction du temps montre que, si la production des fréons -11 et -12 augmente continûment de 3% par an, des diminutions de plus de 10% sont vraisemblables à partir de l'année 2050. Si toutefois le scénario arrête la croissance de la production mondiale à une fois et demie sa valeur de 1985, la perte en ozone ne devrait pas dépasser 4 à 5%. A titre d'exemple, lorsque la production des fréons -11 et -12 augmente de 3% par an jusqu'à ce qu'elle atteigne ce plafond (et reste constante ensuite), que la production de

F-113 s'accroît de 6% par an jusqu'à valoir celle de F-11 (et lui rester égale ensuite) et que les concentrations de  $\text{CO}_2$ ,  $\text{CH}_4$  et  $\text{N}_2\text{O}$  augmentent respectivement de 0,5; 1 et 0,25% par an, la colonne d'ozone se voit réduite de 3,5% en 2040 par rapport à sa valeur un siècle plus tôt. Le calcul prédit une lente restauration après l'an 2080, liée à l'augmentation rapide du méthane.

Le modèle révèle que la perte d'ozone augmente de façon presque linéaire avec la concentration en chlore tant que la fraction molaire de celui-ci reste inférieure à celle de l'azote actif, la sensibilité de l'ozone au chlore restant toutefois fortement dépendante de la concentration en  $\text{NO}_y$ . Si la fraction molaire de  $\text{Cl}_x$  devient comparable ou supérieure à celle de  $\text{NO}_y$ , la diminution d'ozone croît rapidement avec la quantité de chlore dans l'atmosphère.

## Samenvatting

De reactie van de atmosfeer op emissies van chloorfluorkoolstoffen (CFCs), andere chloorkoolstoffen (ClCs) en op verhoogde concentraties van andere stralingsactieve minderheidsgassen zoals  $\text{CO}_2$ ,  $\text{CH}_4$  en  $\text{N}_2\text{O}$ , wordt berekend door middel van een eendimensionaal model dat chemische reacties, stralingsprocessen en verticaal transport combineert. Er wordt aangetoond dat in de hoge stratosfeer belangrijke dalingen in de temperatuur en in de ozonconcentratie moeten verwacht worden voornamelijk als resultaat van een stijgend aantal chlooratomen afkomstig van de fotolyse van de CFCs. In het geval van een constante emissie van de chloorfluorkoolstoffen -11 en -12, ongeveer gelijk aan de waarde van 1980 (309 kT/jaar voor F-11 en 433 kT/jaar voor F-12), en met betrekking tot haar waarde in de preindustriële atmosfeer, daalt de ozonconcentratie  $\pm 60$  tot 70% op 40 km hoogte. De overeenstemmende vermindering van het totaal atmosferisch gehalte (kolom) van hetzelfde gas is 8,7% wanneer de terugwerkende kracht van de temperatuur op de chemie in het model vervat is, en 5,5% wanneer dit niet het geval is. Een verdubbeling van de  $\text{CO}_2$  concentratie leidt tot een stijging van 1,8% in de ozonconcentratie en tot een stijging van 2K in de oppervlaktetemperatuur. Op 40 km stijgt de ozonconcentratie met 15% en de temperatuur daalt met 8K. Bij een verdubbeling van de methaanconcentratie is er een stijging van 2,4% in de ozonconcentratie. Een stijging van 20% in de hoeveelheid  $\text{N}_2\text{O}$  leidt tot een ozonvermindering van 1,4%.

De berekening van de totale hoeveelheid ozon in functie van de tijd toont aan dat, indien de produktie van F-11 en F-12 constant stijgt met 3%/jaar, er waarschijnlijk een daling in de ozonhoeveelheid van meer dan 10% zal zijn na 2050. Indien het scenario echter de groei van de wereldproduktie terugbrengt tot 1,5 maal de waarde van 1985, zou het verlies aan ozon de 4 à 5% niet moeten overschrijden. Bijvoorbeeld als de produktie van F-11 en F-12 met 3%/jaar stijgt, als de produktie van F-113

stijgt met 6%/jaar (maar nooit de produktie van F-11 overschrijdt) en als de concentratie van  $\text{CO}_2$ ,  $\text{CH}_4$  en  $\text{N}_2\text{O}$  toeneemt met respectievelijk 0,5; 1,0 en 0,25%/jaar, is de ozonconcentratie herleid tot 3,5% in het jaar 2040 (vergeleken met de waarde van 1940). Een traag herstel wordt voorspeld na het jaar 2080, te wijten aan een snelle toename van de methaanconcentratie.

Het model toont dat het verlies van ozon bijna lineair stijgt met de chloorconcentratie, zolang de mengverhouding van actieve chloor kleiner blijft dan die van actieve stikstof, waarbij de gevoeligheid van ozon voor chloor sterk afhankelijk blijft van de  $\text{NO}_y$  concentratie. Indien de mengverhouding van  $\text{CL}_x$  vergelijkbaar wordt met of groter wordt dan die van  $\text{NO}_y$ , stijgt de ozonvermindering snel met de hoeveelheid chloor in de atmosfeer.



## Zusammenfassung

Die Reaktion der Atmosphäre auf Chlorfluorkohlenstoffemissionen (CFCs), auf anderen Chlorkohlenstoffen (ClCs) und auf erhöhter Konzentrationen von anderen Strahlungsaktiven Spurengasen wie  $\text{CO}_2$ ,  $\text{CH}_4$  und  $\text{N}_2\text{O}$ , wird berechnet mittels eines eindimensionalen Modelles das chemische Reaktionen, Strahlungsprozessen und vertikalen Transport kombiniert. Man zeigt dass in der Höhe Stratosphäre wichtige Senkungen in der Temperatur und in der Ozonkonzentration erwartet müssen werden vornehmlich als Resultat von einer steigenden Anzahl Chloratomen verursacht durch die Fotolyse der CFCs. Im Fall einer konstanten Emission der CFCs -11 und -12, + gleich am Wert von 1980 (309 kT/Jahr für F-11 und 433 kT/Jahr für F-12), und mit Bezug auf ihrem Wert in der pre-industriellen Atmosphäre, sinkt die Ozonkonzentration  $\pm$  60 bis 70% auf 40 Km Höhe. Die Übereinstimmende Verringerung des atmosphärischen Gesamtgehaltes des selben Gases ist 8,7% wenn die rückwirkende Kraft der Temperatur auf der Chemie im Modell enthalten ist, und 5,5% wenn sie nicht ist. Eine Verdopplung der  $\text{CO}_2$  Konzentration führt zu einer Steigung von 1,8% in der Ozonkonzentration und zu einer Steigung von 2K in der Oberflächentemperatur. Auf 40 Km steigt die Ozonkonzentration mit 15% und die Temperatur fällt mit 8K. Bei einer Verdopplung der Methankonzentration gibt es eine Steigung von 2,4% in der Ozonkonzentration. Eine Steigung von 20% in der Quantität  $\text{N}_2\text{O}$  führt zu einer Ozonverringerung von 1,4%.

Die Berechnung der Gesamtquantität Ozon mit Rücksicht auf der Zeit zeigt dass, wenn die Produktion von F-11 und F-12 beständig steigt mit 3%/Jahr, es wahrscheinlich eine Senkung in der Ozonquantität von mehr als 10% sein wird nach 2050. Wenn aber die Steigung der Weltproduktion zurückgeführt wird zu 1,5 Mal der Wert von 1985, wurde der Verlust an Ozon der 4 oder 5% nicht überschreiten müssen. Zum Beispiel wenn die

Produktion von F-11 und F-12 mit 3%/Jahr steigt, wenn die Produktion von F-113 steigt mit 6%/Jahr (aber niemals die Produktion von F-11 überschreitet) und wenn die Konzentration von  $\text{CO}_2$ ,  $\text{CH}_4$  und  $\text{N}_2\text{O}$  steigt mit respektive 0,5; 1,0 und 0,25%/Jahr, ist die Ozonkonzentration herleitet zu 3,5% im Jahr 2040 (im Vergleich zum Wert von 1940). Eine träge Erhöhung wird vorhersagt nach dem Jahr 2080, zuzuschreiben an einer schnelle Zunahme der Methankonzentration.

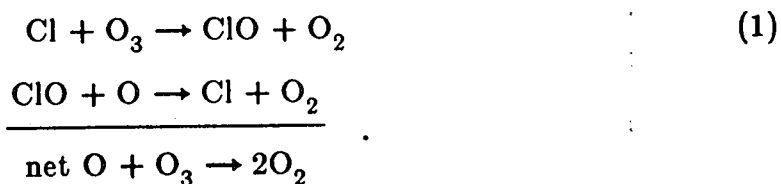
Das Modell zeigt dass der Verlust von Ozon fast linear steigt mit der Chlorkonzentration, wenn das Mischungsverhältnis von aktiven Chlor kleiner bleibt dann das von aktivem Stickstoff, wobei die Empfindlichkeit von Ozon für Chlor stark abhängig bleibt von der  $\text{NO}_y$  Konzentration. Wenn das Mischungsverhältnis von  $\text{Cl}_x$  vergleichbar wird mit oder grösser wird als das von  $\text{NO}_y$ , steigt die Ozonverringeringung schnell mit der Quantität Chlor in der Atmosphäre.

## 1. INTRODUCTION

It is now well recognized that the increase in the concentration of trace gases in the atmosphere such as the chlorofluorocarbons (CFCs), nitrous oxide ( $\text{N}_2\text{O}$ ), methane ( $\text{CH}_4$ ) and carbon dioxide ( $\text{CO}_2$ ), essentially as a result of agricultural practices and industrial activity, should significantly modify the structure of the ozone layer and influence the earth's climate in the future. Among the species which have the potential to perturb the ozone layer in the stratosphere, the chlorofluorocarbons play a major role. These organic molecules are used as aerosol propellants, refrigerants, foam blowing agents, solvents, etc. Those which are important to the ozone issue are produced in relatively large quantity and are stable towards chemical destruction in the troposphere. The species involved are essentially  $\text{CFCl}_3$  (F-11),  $\text{CF}_2\text{Cl}_2$  (F-12). In addition, other important compounds are  $\text{CCl}_4$  (carbon tetrachloride),  $\text{CH}_3\text{CCl}_3$  (methyl chloroform) and to a lesser extent  $\text{CF}_2\text{ClCFCl}_2$  (F-113). Other potential harmful industrial halocarbons such as  $\text{CHClF}_2$  (F-22),  $\text{CBrF}_3$  (Halon 1301) or  $\text{CF}_2\text{ClBr}$  (Halon 1211) play at the present time only a secondary role and will not be considered further. The global emissions of F-11 and F-12 have increased by about 10%/yr until 1974. Since then the release in the atmosphere has been essentially constant, namely about 250-350 kT/yr for F-11 and 350-450 kT/yr for F-12 (CMA, 1985; Fabian, 1986). However, as the lifetime of these 2 compounds is of the order of 80 yrs for F-11 and 170 yrs for F-12, their concentration in the stratosphere has continued to increase. Large uncertainties exist in the

quantitative values associated with the budget of  $\text{CCl}_4$ . According to a recent study by Simmonds et al. (1983), the emission of carbon tetrachloride should be of the order of 100 kT/yr and its global lifetime close to 75 yrs. The emission rate of methyl chloroform in the atmosphere (expressed in mass units) appears to be more than twice that of F-11 and F-12 and is growing by about 16%/yr (Fabian, 1986). However, according to Logan et al. (1981), about 70% of the sink of this gas (essentially by OH) takes place in the troposphere, so that the lifetime of  $\text{CH}_3\text{CCl}_3$  is of the order of 7 yrs (Rasmussen and Khalil, 1981a).

The only important natural source of chlorine atoms appears to be through methyl chloride ( $\text{CH}_3\text{Cl}$ ) which is produced by the oceans, by biomass burning and by fungi (Harper, 1985). A range of 1350-9000 kT/yr is quoted by Fabian (1986), based on estimates by Cicerone et al. (1975), Yung et al. (1975), Singh et al. (1979), Graedel (1979) and Crutzen et al. (1979). Figure 1 shows the contribution of the various organic chlorine compounds to the production rate of inorganic chlorine for conditions corresponding to year 1980. The chlorine atoms resulting from the dissociation of the chlorocarbons (ClCs) destroy ozone through the catalytical cycle (Stolarski and Cicerone, 1974)



In the preindustrial atmosphere, the mixing ratio of total inorganic chlorine (essentially in the form of Cl, ClO,  $\text{ClONO}_2$ , HCl and HOCl) was close to 0.7

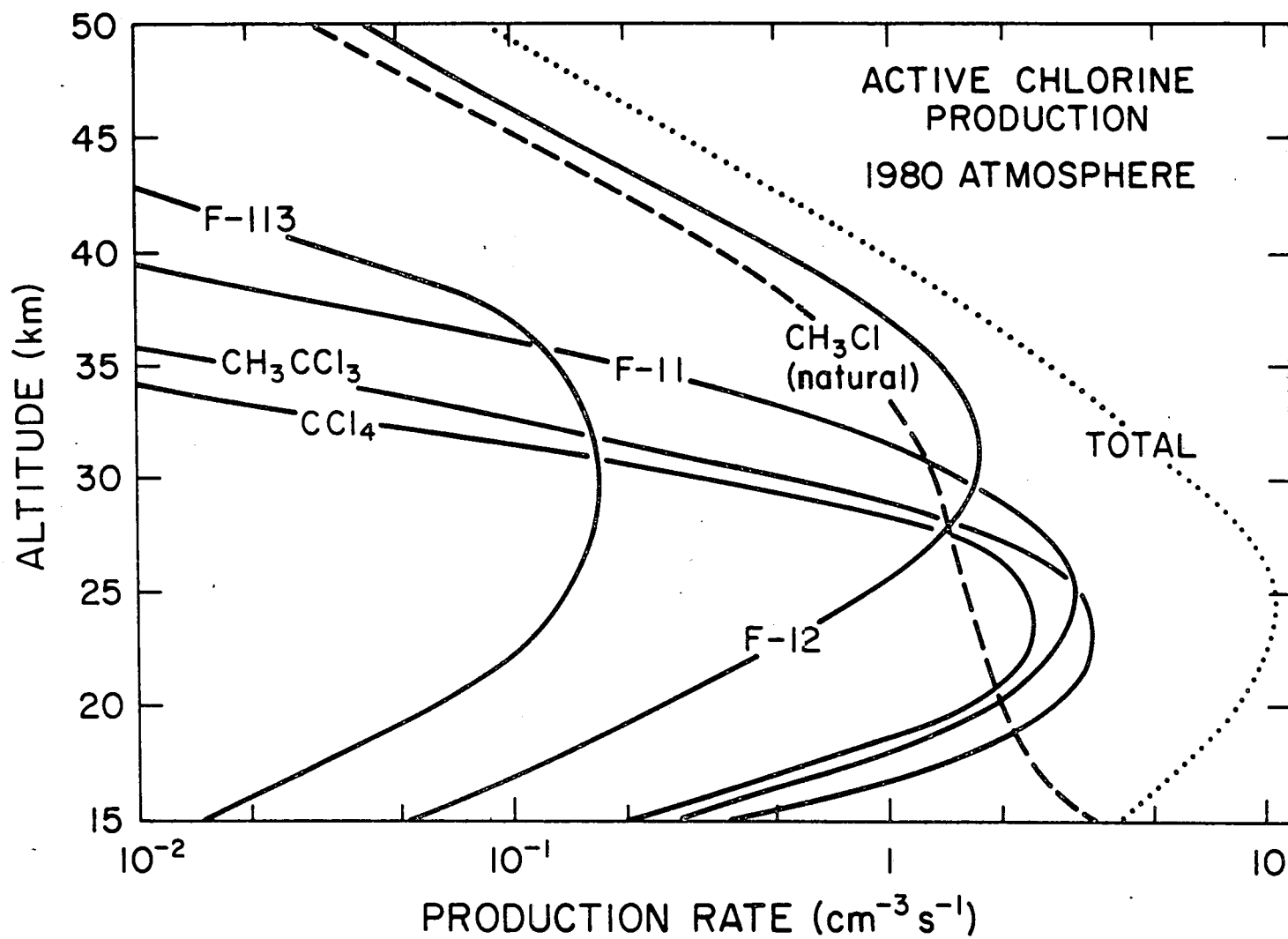
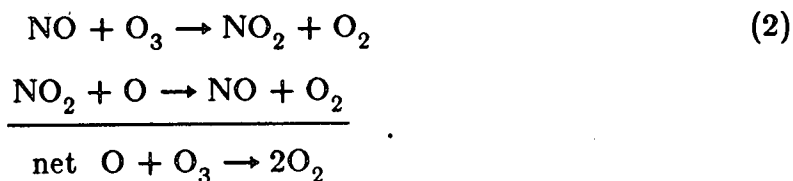


Fig. 1.- Contribution of natural  $\text{CH}_3\text{Cl}$  and man-made chlorocarbons to the production rate of active chlorine in the stratosphere (1980 reference atmosphere).

ppbv, as a result of the destruction of the naturally produced methyl chloride. It is presently of the order of 2.5-2.8 ppbv in the upper stratosphere (WMO/NASA, 1986).

Nitrous oxide ( $N_2O$ ), which has a current surface mixing ratio of 307 ppbv (Rasmussen and Khalil, 1986), is the main source of nitrogen oxides in the stratosphere. It is produced by biological processes, mostly by bacterial nitrification and denitrification, and by fossil fuel and biomass combustion. Its growing concentration (annually about 0.2-0.3%, Weiss, 1981; Khalil and Rasmussen, 1983; Rasmussen and Khalil, 1986) is believed to be largely associated with human activity. Nitric oxide resulting from its destruction by electronically excited oxygen atoms (Nicolet, 1971; Crutzen, 1971) is responsible for what is known to be the most efficient ozone destruction mechanism in the stratosphere (Crutzen, 1970) by the following catalytical cycle



Methane ( $CH_4$ ) is the most abundant hydrocarbon in the atmosphere. Its present mixing ratio at the surface is about 1.7 ppmv in the Northern Hemisphere (Rasmussen and Khalil, 1986; WMO/NASA, 1986). A substantial increase in the concentration of this gas has been observed by Rasmussen and Khalil (1981b) [ $(2 \pm 0.5)\%/yr$ ], by Blake et al. (1982) [ $1.5 \pm 0.5\%/yr$ ] and by Rasmussen and Khalil (1986) [ $(17.5 \pm 1.3) \text{ pptv/yr}$ ]. This molecule initiates a

complex chemistry which is capable of altering the concentration of other radiatively active trace gases. For example, the oxidation of methane produces, when the amount of nitrogen oxides is sufficiently large, ozone molecules, especially in the troposphere (Crutzen, 1974; 1986). Moreover, one of the end products of this oxidation chain is water vapor which is also radiatively active. The increase in the methane content should also modify the distribution of hydroxyl radicals with subsequent effects on the chemistry of other species. Such perturbations of OH should modify the photooxidation rates of several natural and anthropogenic species and affect the lifetime of trace gases that pass from the earth's surface to the troposphere and the stratosphere (Thompson and Cicerone, 1986). Finally the ratio between the concentration of ClO (which directly affects ozone) and HCl (which is a chlorine reservoir without chemical influence on ozone) is significantly affected by the methane content.

Carbon dioxide is chemically very stable in the entire atmosphere below 80 km altitude. Its mixing ratio is thus essentially uniform below this level with a current value close to 350 ppmv. Continuous monitoring of the CO<sub>2</sub> concentration (Keeling, 1983) has shown an increase since 1958 of the order of 0.2-0.3%/yr, probably resulting in large part from combustion processes (coal, oil, natural gas) and land-use changes (deforestation, burning, etc...). Table 1 summarizes the characteristics of the trace gases with potentially important chemical, radiative and climatic effects, which are considered in the present study.

**Table 1**  
**Main characteristics of the chemical species involved in the present study (source gases only)**  
**1980 conditions**

Species	Typical mixing ratio at the surface	Integrated concentration above the surface (cm <sup>-2</sup> )	Total atmospheric mass (MT)	Total annual destruction (kT/yr)	Calculated lifetime (yrs)	Recent growth rate (%/yr)
CO <sub>2</sub>	340 ppmv	6.1 × 10 <sup>21</sup>	2.1 × 10 <sup>6</sup>			0.2-0.5
CH <sub>4</sub>	1.6 ppmv	3.0 × 10 <sup>19</sup>	4 183	6.38 × 10 <sup>5</sup>	6.5	1-2
N <sub>2</sub> O	300 ppbv	5.8 × 10 <sup>18</sup>	2 170	1.22 × 10 <sup>4</sup>	177	0.25
CH <sub>3</sub> Cl	700 pptv	1.2 × 10 <sup>16</sup>	5.27	5.38	1	—
CCl <sub>4</sub>	100 pptv	1.9 × 10 <sup>15</sup>	2.44	35	69	0-3
CH <sub>3</sub> CCl <sub>3</sub>	100 pptv	1.8 × 10 <sup>15</sup>	2.09	480	4	5-8
F-11	170 pptv	3.2 × 10 <sup>15</sup>	3.74	42.6	88	5-8
F-12	285 pptv	5.5 × 10 <sup>15</sup>	5.65	33.9	167	5-8
F-113	22 pptv	4.2 × 10 <sup>14</sup>	0.67	4.99	134	15-20



Model calculations reported for example in the WMO/NASA (1986) report predict a steady-state ozone depletion of 5-9 percent for a constant anthropogenic production of chlorocarbons (CICs) at the present level and neglecting the effect of increasing concentrations of other trace gases such as CO<sub>2</sub>, CH<sub>4</sub> and N<sub>2</sub>O. Moreover, as noted recently by Ramanathan et al. (1985) and by Dickinson and Cicerone (1986), the continuous additions of trace species during the next 65 years are predicted to cause the global surface temperature to rise by between 1 and 5 K.

Predictions of future changes in atmospheric ozone and temperature require coupled models which simultaneously and interactively represent the chemical and the radiative behavior of the atmosphere and its response to human perturbations. The purpose of this paper is to investigate these effects. The response of the atmosphere to the emissions of trace gases has been extensively studied in recent years (see e.g., Wang et al., 1976; 1986; Wang and Molnar, 1985; Ramanathan, 1976; Ramanathan et al., 1985; 1986; Donner and Ramanathan, 1980; Lacis et al., 1981; Wuebbles, 1983; Callis et al., 1983; Wuebbles et al., 1983; Brasseur, 1984; Brasseur et al., 1985; de Rudder and Brasseur, 1985; Bruehl and Crutzen, 1984; Owens et al., 1985; Solomon et al., 1985; Isaksen and Stordal, 1986; Dickinson and Cicerone, 1986; Connell and Wuebbles, 1986; Tricot and Berger, 1986; and others). Some of these papers have either studied the chemical sensitivity of ozone to changes in the amount of injected "source gases" (parameterizing crudely the radiative feedbacks and,

in certain cases, ignoring the climatic impact at the earth's surface) or considered the pure radiative and climatic response of the injection in the atmosphere of "greenhouse gases" (neglecting chemical feedbacks). In this work, all effects will be treated interactively through a coupled one-dimensional time-dependent chemical-radiative-transport model. This model, which is described in section 2, is used (section 3) to calculate to predict future changes in the ozone content and in the temperature, based on several possible time-dependent scenarios of future atmospheric emissions. The sensitivity of the atmospheric responses to the values adopted for parameters such as the eddy diffusion coefficient for vertical transport and the atmospheric budget of nitrogen oxides is estimated and discussed in section 4.

## 2. THE MODEL

### 2.1 Model description

The model used in the present study is one-dimensional and extends from the earth's surface to the altitude of 100 km, although the temperature is calculated only up to 60 km and kept fixed above 70 km (with a linear transition between 60 and 70 km). The vertical distribution of the trace gases is calculated by solving continuity/transport equations

$$\frac{\partial X_i}{\partial t} - \frac{1}{[M]} \frac{\partial}{\partial z} \left( K [M] \frac{\partial X_i}{\partial z} \right) = S_i \quad (3)$$

with appropriate boundary conditions. In this expression  $X_i$  is the volume

mixing ratio of species  $i$ ,  $[M]$  the atmospheric density,  $t$  the time and  $z$  the altitude. The vertical eddy diffusion coefficient  $K$  parameterizes the strength of the net vertical exchanges. Its value is of the order of  $(1-2) \times 10^5 \text{ cm}^2 \text{ s}^{-1}$  in the troposphere and  $(0.5-5) \times 10^4 \text{ cm}^2 \text{ s}^{-1}$  in the stratosphere. The profile adopted in most numerical simulations in this work is identical to the profile used by Wuebbles (private communication, 1985) and is shown in Figure 2. The source term  $S_i$  is estimated taking into consideration the formation and the destruction of each species  $i$  by chemical and photochemical reactions.

In order to avoid numerical problems due to the "stiffness" of the system of equations due to the very broad spectrum of lifetimes associated with the different chemical constituents, some of the species with strong chemical couplings are grouped and equation (1) is applied to the "chemical family" as a whole instead of to each individual constituent. For the most reactive compounds, photochemical equilibrium conditions are applied. The system is then solved for the species belonging to the oxygen-hydrogen-carbon-nitrogen-chlorine families, using an implicit numerical method. The adopted boundary conditions applied for the 1980 reference atmosphere are identical to the conditions used in the WMO/NASA report and are specified in Table 2. For perturbed cases, the boundary conditions of source gases are adapted to account for increasing mixing ratios or fluxes at the surface. Concentrations of ozone and nitrogen oxides are allowed to vary in the troposphere since a deposition velocity is specified for these species at the lower boundary. The chemical rate constants required to

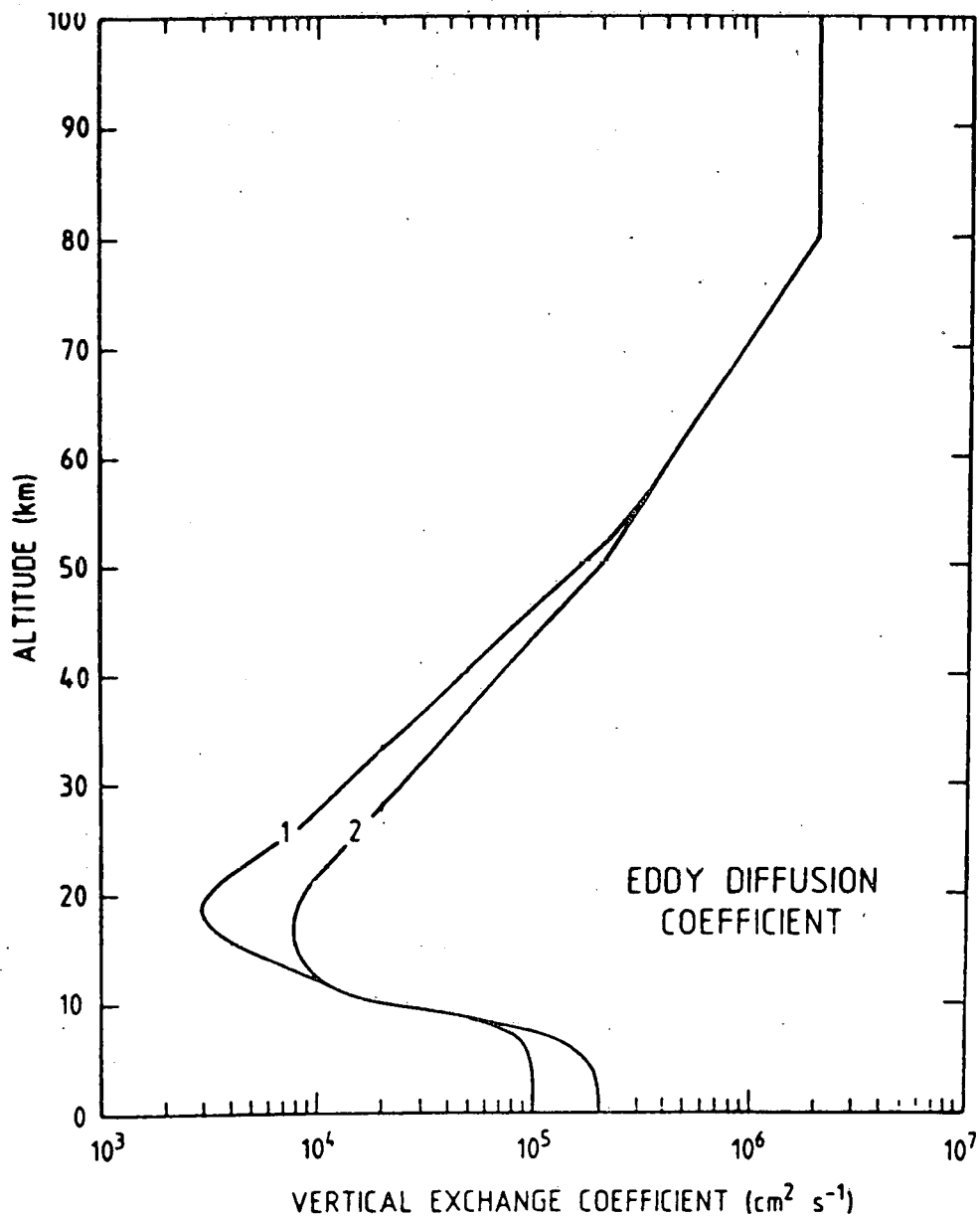


Fig. 2.- Vertical distribution of eddy diffusion coefficients. Profile 1 (Wuebbles, private communication) is used in all model calculations unless otherwise specified. Profile 2 is considered only for sensitivity purposes.

**Table 2**  
**Boundary conditions adopted in the model to**  
**describe the 1980 atmosphere**

Species	Lower Boundary	Upper Boundary
N <sub>2</sub> O	X = 300 ppbv	Φ = 0
CH <sub>4</sub>	X = 1.6 ppmv	Φ = 0
CH <sub>3</sub> Cl	X = 700 pptv	Φ = 0
CCl <sub>4</sub>	X = 100 pptv	Φ = 0
CFCl <sub>3</sub> (F-11)	X = 170 pptv	Φ = 0
CF <sub>2</sub> CCl <sub>2</sub> (F-12)	X = 290 pptv	Φ = 0
CF <sub>2</sub> Cl-CFCl <sub>2</sub> (F-113)	X = 22 pptv	Φ = 0
CH <sub>3</sub> CCl <sub>3</sub>	X = 100 pptv	Φ = 0
CO	X = 100 ppbv	Φ = 0
Cl <sub>x</sub>	X = 1 ppbv	Φ = 0
NO <sub>y</sub>	w <sub>D</sub> = -0.5 cm/s	X = 5.4 ppbv
O <sub>x</sub>	w <sub>D</sub> = -0.1 cm/s	X = 5.3 × 10 <sup>-2</sup>
H	X = 0	X = 4.3 ppbv

X = mixing ratio

Φ = vertical flux

w<sub>D</sub> = deposition velocity

calculate the source terms are taken from the JPL compilation (DeMore et al., 1985). The photodissociation frequency of the molecules is calculated with the solar irradiance compiled by Brasseur and Simon (1981). The solar penetration in the region of the Schumann-Runge bands of molecular oxygen, as well as the photodissociation rate of  $O_2$  in the same spectral range, are derived using the method of Kockarts (1976). The photodissociation coefficient of NO is calculated with the formula of Nicolet (1979). The absorption cross-sections of  $O_2$  in the Herzberg continuum are taken from the *in-situ* measurements by Herman and Mentall (1982). The diurnal average of the photodissociation coefficients is approximated by a 4 point integral between sunrise and sunset (see Cunnold et al., 1975). The water vapor mixing ratio in the stratosphere is specified such that the mixing ratio of hydrogen contained in  $H_2O$ ,  $CH_4$  and  $H_2$  is constant with altitude. The water vapor profile is thus changing as the methane distribution is modified.

The code used to calculate the vertical distribution of the temperature has been developed by Ramanathan (1976), Donner and Ramanathan (1980), and Kiehl and Ramanathan (1983) and modified by Bruehl (1986). It has been recently used by Bruehl and Crutzen (1984) to investigate the effects of greenhouse gases on atmospheric ozone and temperature.

The calculated heating rate resulting from the absorption of solar radiation involves the effect of ozone, nitrogen oxide, water vapor and carbon dioxide. The heating by ozone and nitrogen dioxide is obtained from a detailed spectral

integration involving the relevant absorption cross sections and solar irradiance. The heating by water vapor in the stratosphere is calculated according to the unpublished method of Ramanathan (see Bruehl, 1986). The contribution of the heating by CO<sub>2</sub> is derived from a computation based on the broadband absorptance method expressed by Kiehl et al. (1985) for the 1.4 μm, 1.6 μm, 2.7 μm and 4.3 μm bands. A total of 30 bands are included, based on the measurements of Yamanouchi (1977).

The radiative effect of the 15 μm band of CO<sub>2</sub> is estimated by the broadband model of Kiehl and Ramanathan (1983). Total overlap is assumed for 56 "hot" and isotopic bands. In the upper stratosphere, the transition from the Lorentz to the Doppler regime is performed by choosing the maximum cooling associated with these 2 lineshapes (Ramanathan, 1976). The temperature dependence of the line parameters is fully included. A broadband absorptance model with the related parameters specified by Ramanathan and Dickinson (1979) is adopted for the two bands of ozone near 9.6 μm. Again, the maximum cooling method is used to discriminate between Lorentz and Doppler regimes in the upper stratosphere. For water vapor, the contribution of the vibration-rotation and pure rotation spectra is represented by the emissivity method of Ramanathan (1976), supplemented by data of Rogers and Walshaw (1966). The fit of Roberts et al. (1976) is used for the water vapor continuum. Its contribution however is neglected in the stratosphere.

The broadband absorptance method of Ramanathan is used for methane and nitrous oxide with the data of Donner and Ramanathan (1980). In the case of the  $N_2O$  band at  $16.9 \mu m$ , two "hot" bands are considered simultaneously with the fundamental band. The overlap with the  $CO_2$  and the  $H_2O$  spectra is treated as in Kiehl and Ramanathan (1983). For the  $7.7 \mu m$  fundamental and hot bands, the intensities are taken from McClatchey et al. (1973). Overlap with  $H_2O$  and  $CH_4$  bands as well as temperature dependences of the spectral parameters are fully included. The radiative transfer associated with the F-11 and F-12 molecules includes four bands for each constituent with intensities and band widths taken from Kagann et al. (1983).

This model, called code C1, is run iteratively until radiative equilibrium conditions are reached in the stratosphere. In the troposphere, a convective adjustment is performed such that the lapse rate never exceeds  $-5.9 K/km$ . The surface temperature is obtained by an iterative procedure until an energy balance between incoming and outgoing radiation is achieved at the top of the atmosphere. Clouds are included with a top altitude of 4 km and a global coverage equal to 55% of the earth's area. For the 1980 atmosphere, in which the chemistry is self-consistently calculated, the surface temperature calculated in the model is 288.9 K. The incoming solar energy is  $341.65 Wm^{-2}$  and the outgoing short-wave energy is  $109.28 Wm^{-2}$ , corresponding thus to a planetary albedo of 32 percent.



It should be noted that the interaction between the atmosphere and the ocean is not included in the radiative code. Because of its large heat capacity, the ocean delays significantly the response of the surface temperature to perturbations in the concentration of precursor gases. Models, which intend to simulate explicitly the transient response of the earth's climate, usually consider 3 or more thermal reservoirs (e.g., the atmosphere, the surface mixed layer of the ocean and the deep ocean) and parameterize the heat transfer between these reservoirs (see e.g., Dickinson, 1981). Therefore, changes in the surface temperature will be assessed only for steady-state cases. Time history of the temperature will be reported only above 20 km, where the effect of the thermal inertia provided by the ocean is small.

In order to investigate the dependence of the results on the adopted radiative scheme, some of the calculations to derive the vertical temperature profile have been repeated using another numerical code (called C2). In this second model, which was used in the earlier work of Brasseur et al. (1985), the heating rate is calculated according to the formulation of Schoeberl and Strobel (1978). The infrared code (Morcrette, private communication, 1983), derives average parameterized transmission functions for 4 broad wavelength intervals (15  $\mu\text{m}$   $\text{CO}_2$ , 9.6  $\mu\text{m}$   $\text{O}_3$ , rotational and 6.3  $\mu\text{m}$   $\text{H}_2\text{O}$  bands and the atmospheric window) and takes into account the overlapping of several bands as well as the temperature and pressure effects on the spectral parameters. This parameterization of the transmission functions is based on a more detailed model including

116 intervals. The radiative effects of trace gases other than  $O_3$ ,  $H_2O$  and  $CO_2$  are not included. A more detailed description of the radiative transfer code is given in Brasseur et al. (1985). The vertical exchanges of heat are parameterized using a first-order closure scheme with an eddy thermal diffusion coefficient (Liou and Ou, 1983). This coefficient is largest in the troposphere, where convective instability occurs, and is several orders of magnitude smaller in the stratosphere, where radiative equilibrium conditions are almost achieved. With values of the eddy thermal diffusion equal to 1.2 times the value of the exchange coefficient used for the vertical transport of the chemical species, the temperature profile is in reasonably good agreement with average observed values. Calculations with this code are performed for a global cloud cover of 50% and a top altitude of 5 km. A fixed relative (rather than absolute) humidity in the troposphere is adopted following Manabe and Wetherald (1967). When perturbation calculations are performed, the surface temperature in this model is kept fixed. This should not significantly affect the calculated temperature changes in the upper stratosphere where radiative equilibrium is achieved but could introduce some errors in the temperature of the lower stratosphere, where the radiative lifetime is significantly longer.

## 2.2 Model results for the reference atmosphere (1980)

Some of the model results for the 1980 reference atmosphere will now be presented in order to validate the model and to point out some unresolved questions in the chemistry of the stratosphere. Figure 3 shows the different

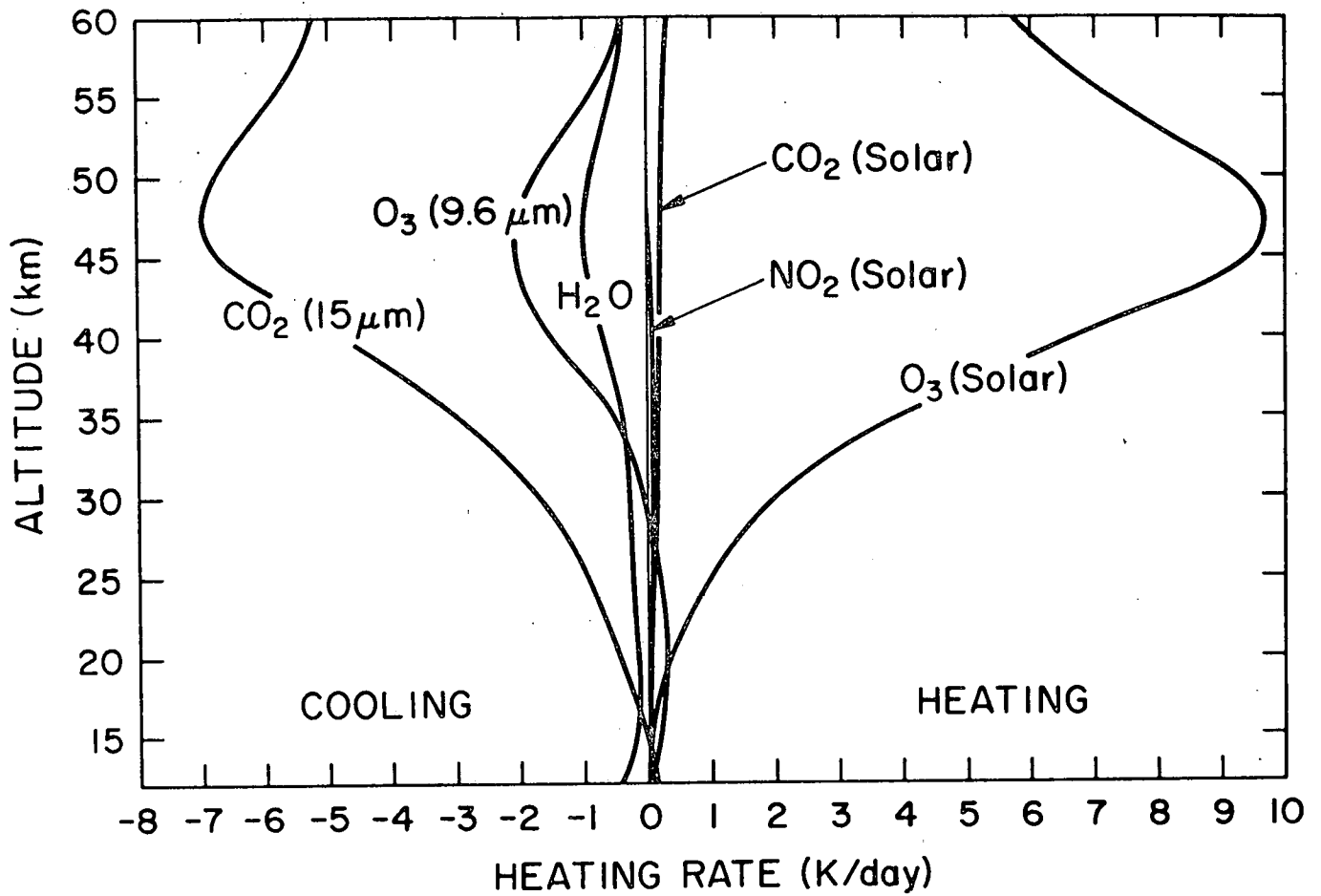


Fig. 3.- Contribution of different trace gases to the heating by short-wave solar radiation and cooling by long-wave terrestrial radiation of the atmosphere between 12 and 60 km altitude. The contribution of CH<sub>4</sub>, N<sub>2</sub>O and the CFCs is too small to be visible on the figure.

components of the heating rate (solar radiation) and the cooling rate (terrestrial radiation) calculated by model C1. The largest contribution for the heating arises from ozone with a maximum of the order of 10 K/day near the stratopause. This effect is almost entirely balanced by the cooling resulting from the infrared emissions by  $\text{CO}_2$ ,  $\text{O}_3$  and  $\text{H}_2\text{O}$ . In the lower stratosphere, all contributions are significantly smaller so that the radiative lifetime becomes considerably longer. This lifetime has been estimated by Brasseur et al. (1986) to be 3 days at 50 km, 9 days at 40 km and 17 days at 30 km. Gille and Lyjak (1986), from an analysis of the LIMS data (observations taken from the Nimbus 7 satellite), have derived radiative relaxation times of 8 days at 40 km, 22 days at 30 km, 40 days at 25 km and about 90 days at 20 km.

The assumption of radiative equilibrium in the lower stratosphere, made in all radiative-convective models (including C1) is approximate and introduces a severe limitation in these types of models. In fact, around and especially just above the tropopause, heat may be transported either horizontally or vertically. Such processes, however, can only be correctly treated in multidimensional models with a detailed description of the dynamics near the tropopause. The response of the temperature and consequently of ozone (as its chemistry is temperature dependent) in the lower stratosphere, derived by purely radiative models, might be inaccurate as the dynamical effects are not taken into account. In models such as C2, some vertical transport of heat is possible through eddy diffusion processes. However, it is not known how the exchange

coefficients are affected by the perturbations (dynamical feedback) to be considered later in this paper.

The vertical profiles of the temperature obtained by both models with the same chemical composition are shown in Figure 4. Despite the numerous differences between these 2 models, the results are both in fairly good agreement with the U.S. Standard Atmosphere (1976). In the lower stratosphere, however, the profiles are significantly different. Indeed, with the formulation of code C1, the transition between the radiative and the convective regimes is sharp. In code C2, the diffusive formulation produces a much smoother transition between the troposphere and the stratosphere and a higher temperature minimum.

The vertical distribution of some of the source gases which are radiatively active is shown in Figures 5.a and 5.b. These profiles are calculated by the model (including temperature feedback with code C1), using the boundary conditions representative of 1980 conditions. When compared to observations (see WMO/NASA, 1986), the distribution of  $N_2O$  is in good agreement with most data observed by *in situ* techniques. In the case of methane, the theoretical curve fits the measurements based on infra-red absorption techniques by Ackerman et al. (1978) but is in disagreement (factor 2 at 40 km) with the values derived from the observations by the SAMS instrument on board the Nimbus 7 satellite (Jones and Pyle, 1984). For the chlorocarbons, the agreement between theory and observations is reasonably good in the case of F-12 and F-113 but the mixing ratios provided by the model above 20 km altitude are higher (factor

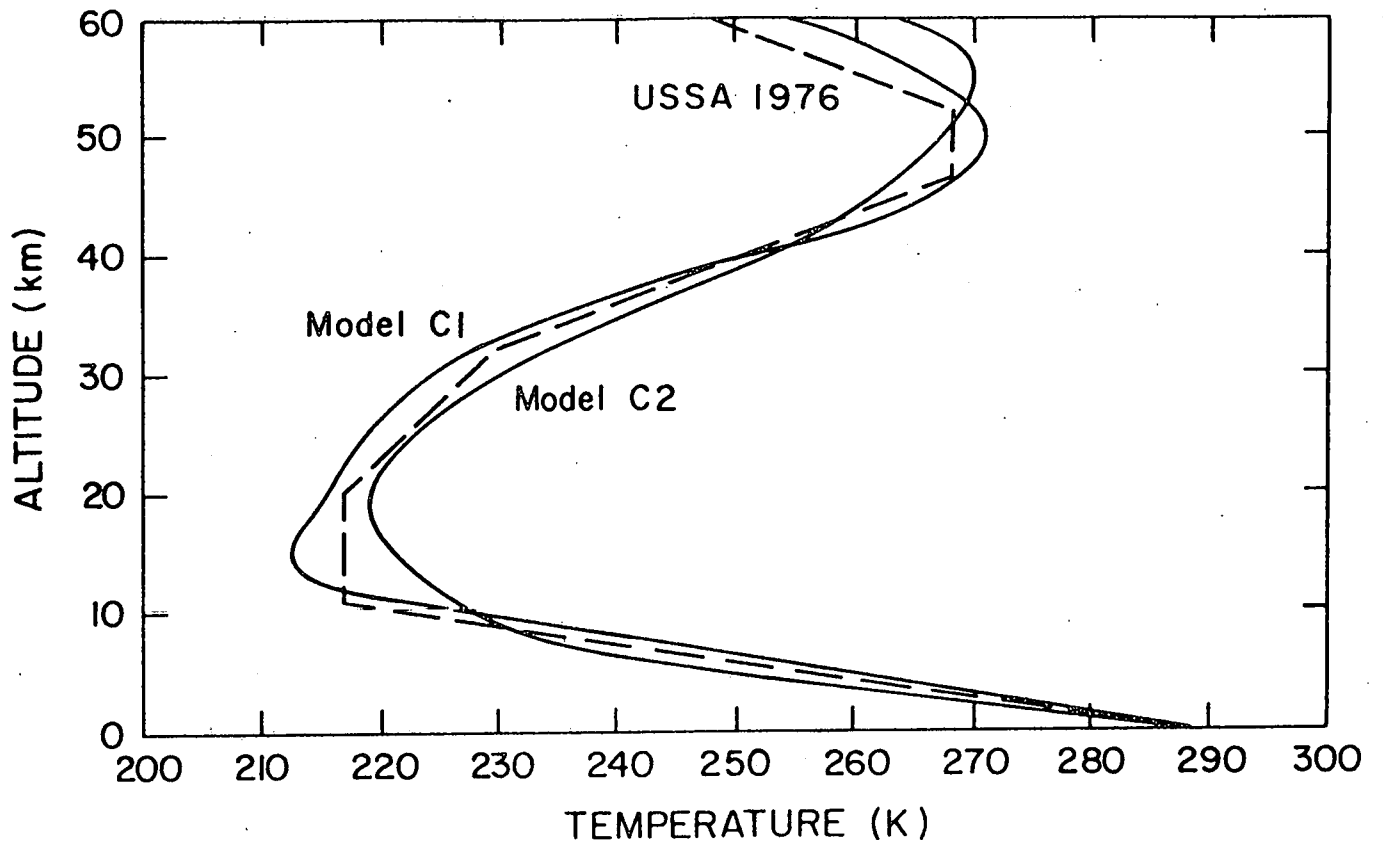


Fig. 4.- Vertical distribution, between 0 and 60 km, of the temperature calculated by two different radiative codes (C1 and C2) and compared to the mean temperature profile of the US standard atmosphere (1976).

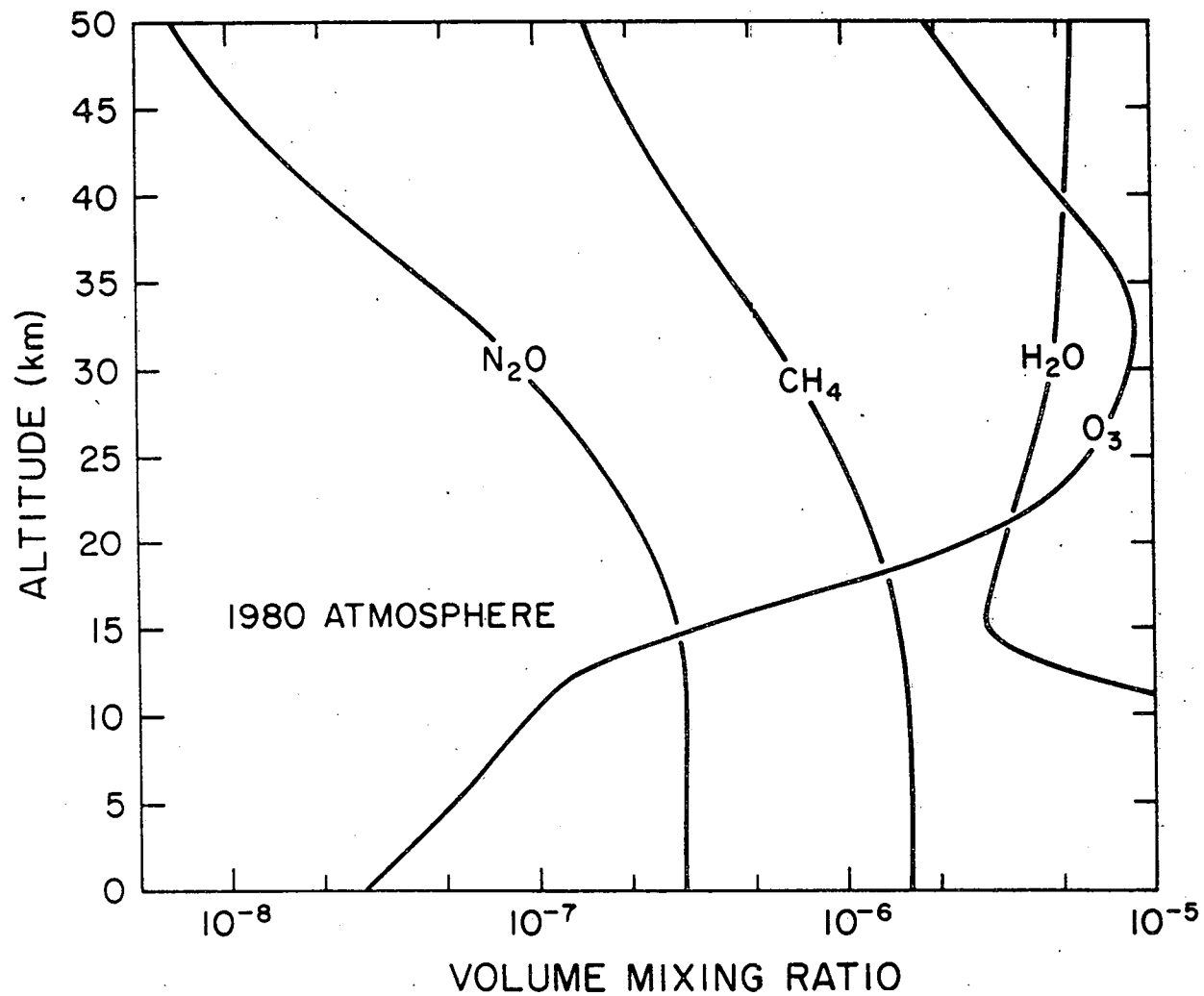


Fig.5a.- Vertical distribution, between 0 and 50 km, of the mixing ratio of radiatively active gases, as computed by the 1-D model for 1980 conditions. Among the chlorocarbons, only F-11 and F-12 are included in the infrared code (C1).

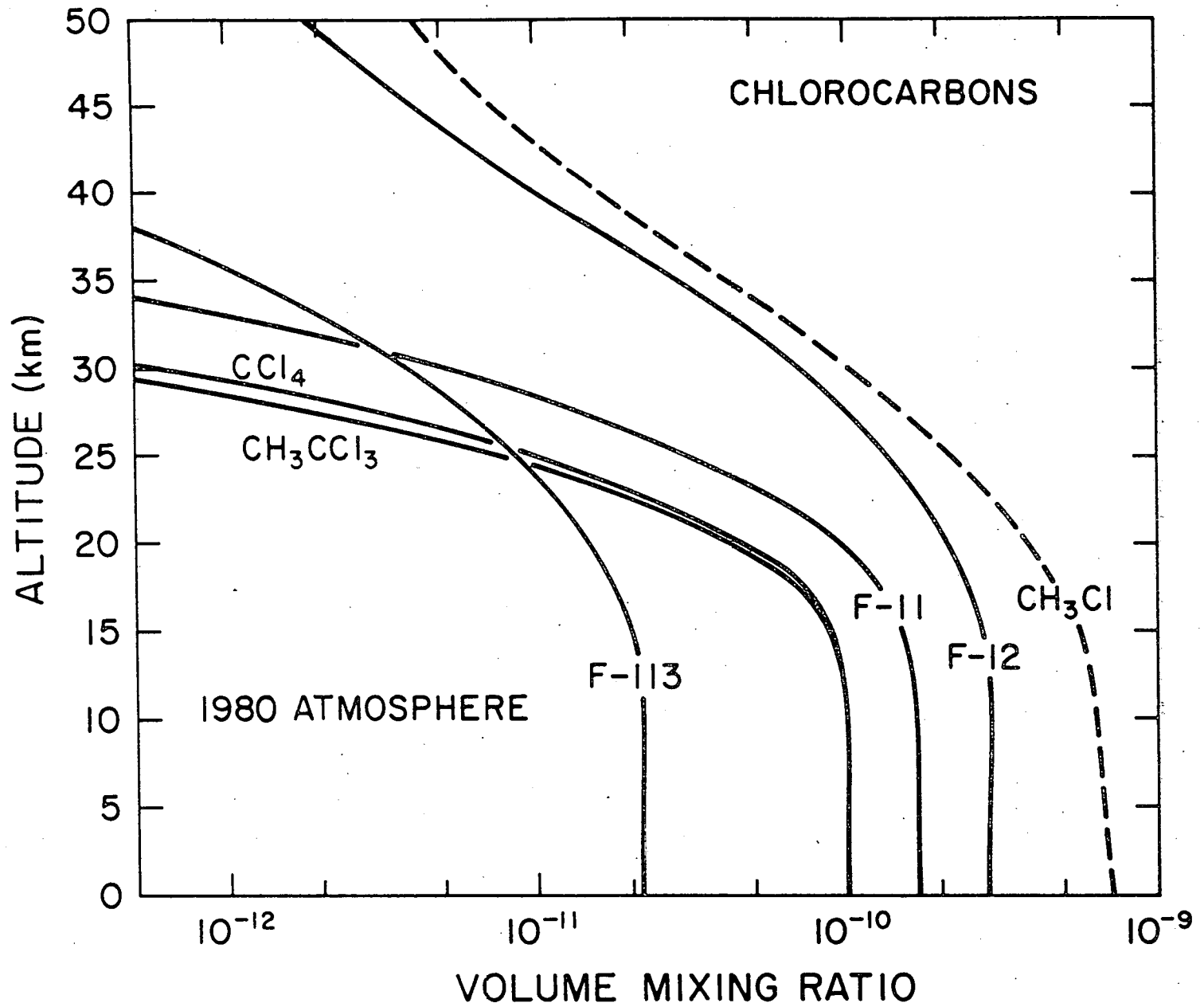


Fig. 5b.-



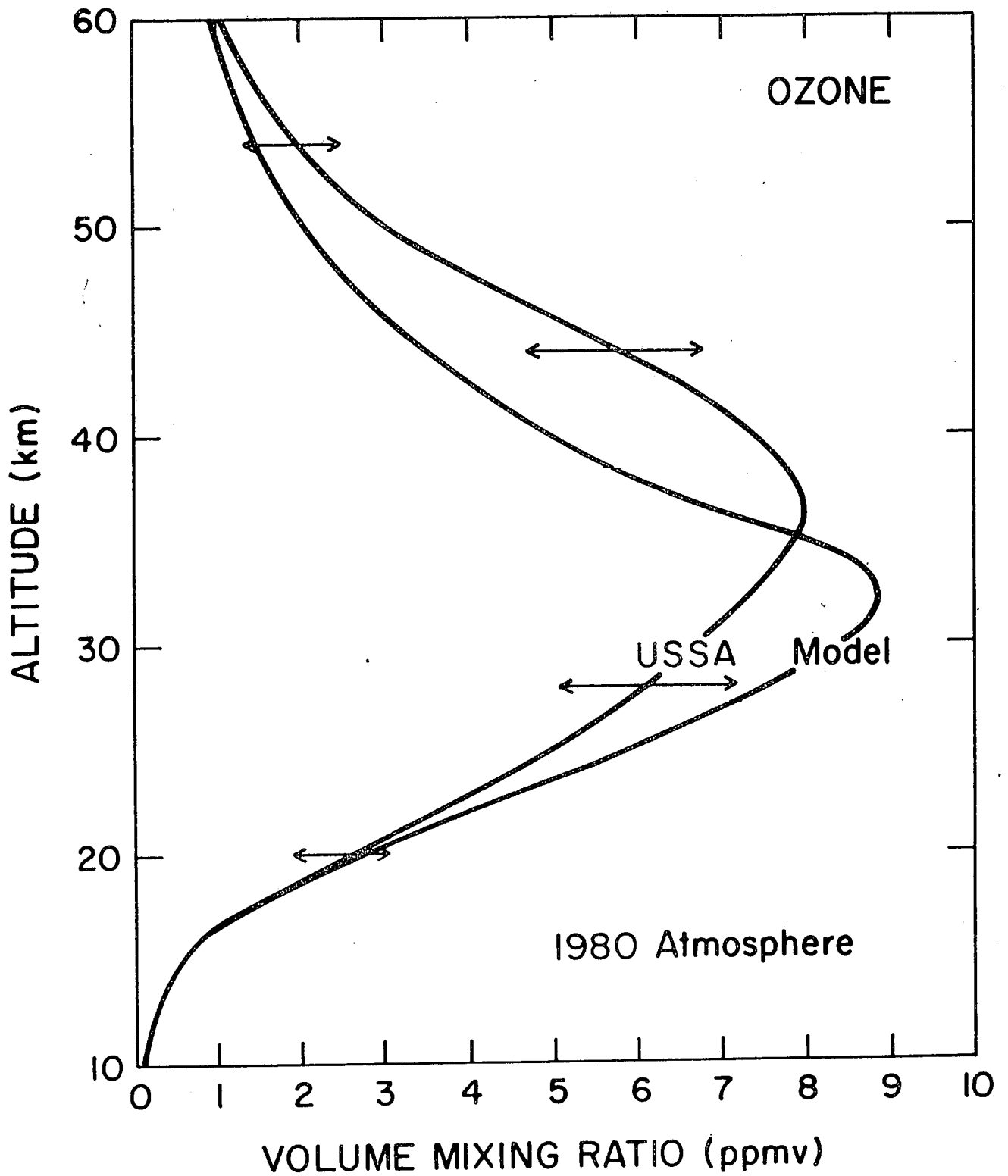


Fig. 6.- Vertical distribution between 10 and 60 km of the ozone mixing ratio calculated by the model for 1980 conditions and compared to the mean profile of the US standard atmosphere (1976).

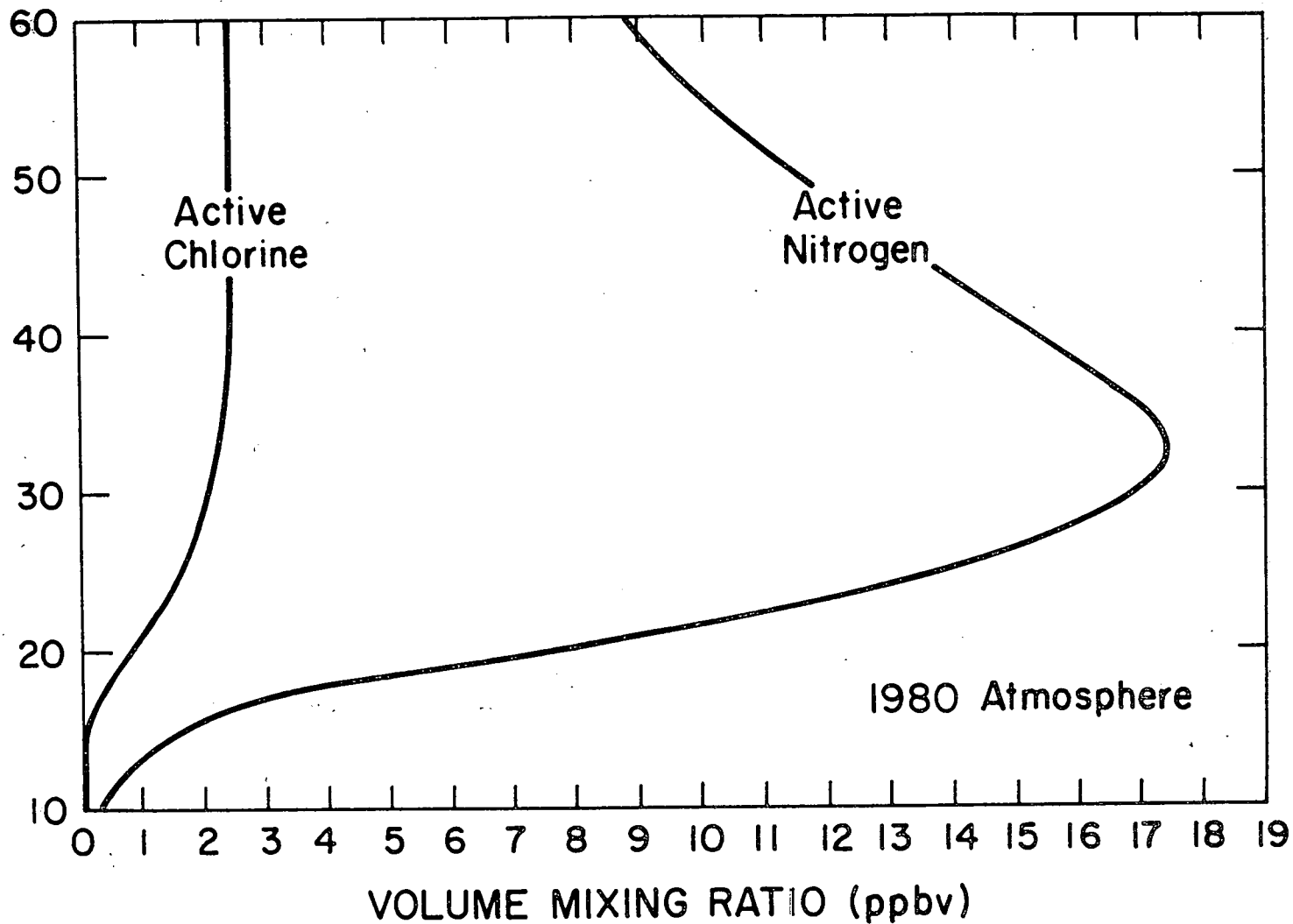


Fig. 7.- Vertical distribution between 10 and 60 km of the active chlorine ( $\text{Cl} + \text{ClO} + \text{HCl} + \text{ClONO}_2 + \text{HOCl}$ ) and of active nitrogen ( $\text{NO} + \text{NO}_2 + \text{NO}_3 + 2\text{N}_2\text{O}_5 + \text{HNO}_3 + \text{HNO}_4 + \text{ClONO}_2$ ) calculated for 1980 conditions.

3 at 25 km) than the *in situ* observations for F-11. The same is true for  $\text{CCl}_4$  and  $\text{CH}_3\text{CCl}_3$ . Similar disagreements are found in essentially all other 1-D models (see WMO/NASA, 1986), indicating that either all destruction processes of some halocarbons have not yet been identified or that the vertical transport of these species is not sufficiently well parameterized. Holton (1986) has shown recently that a proper one-dimensional representation of the vertical exchanges of chemical species requires for each constituent an eddy diffusion coefficient depending on the chemical lifetime of this particular species. In this work, as in all other models presently available, the same eddy diffusion profile has been used for all species (Figure 2). This question should be addressed in the future.

The vertical distribution of the ozone mixing ratio is represented in Figure 6. When compared with observed data (WMO/NASA, 1986), this curve provides concentration values which are 20-30% lower than the measured values in the photochemically controlled region between 35 and 50 km. The possible causes for this discrepancy, which are discussed in detail in the WMO/NASA report (1986), could be associated either with uncertainties in some rate constants of the  $\text{HO}_x$  or  $\text{NO}_x$  chemical schemes or with missing chemistry. The concentrations calculated in the lower stratosphere should be considered as approximate average values since a more realistic representation requires a multidimensional calculation involving a detailed dynamical representation. Indeed, in this region of the atmosphere, the chemical lifetime of ozone exceeds the dynamical lifetime, so that the transport associated especially with

planetary waves plays a dominant role.

As will be discussed below, the chemical balance of ozone and thus its sensitivity to perturbations by chemical compounds released in the atmosphere depend directly on the amount of the total number of active nitrogen atoms ( $\text{NO}_y = \text{NO} + \text{NO}_2 + \text{NO}_3 + 2x\text{N}_2\text{O}_5 + \text{ClONO}_2 + \text{HNO}_3 + \text{HNO}_4$ ) and of active chlorine atoms ( $\text{Cl}_x = \text{Cl} + \text{ClO} + \text{HCl} + \text{ClONO}_2 + \text{HOCl}$ ) which are present in the atmosphere. The modeled vertical distributions of  $\text{NO}_y$  and  $\text{Cl}_x$  for 1980 conditions are displayed in Figure 7. The model provides a mixing ratio for  $\text{NO}_y$  which reaches a maximum of 17.4 ppbv at 33 km. This value is in good agreement with other 1-D models but is 30-50% lower than the maximum value deduced from the LIMS data (Nimbus 7 satellite) by Callis et al. (1985). Ko et al. (1986) have shown recently on a basis of a two-dimensional model that upward transport of nitrogen oxides produced by lightning in the tropical troposphere ( $\sim 2-4 \cdot 10^6 \text{ t N/yr}$ ) could significantly enhance the concentration of  $\text{NO}_y$  in the stratosphere. In this model a production of  $1 \times 10^6 \text{ t N/yr}$  has been assumed to be uniformly distributed between the surface and 10 km altitude. In the case of  $\text{Cl}_x$ , a mixing ratio of 2.4 ppbv is obtained at 50 km. This value is close to the mixing ratio determined by Connell (1986) but is slightly smaller than what seems to result from the observation of the different species belonging to the  $\text{Cl}_x$  family and in particular of its most abundant constituent, namely HCl.

In conclusion, although the agreement between observed and calculated distributions of trace species is fairly good for a number of chemical constituents, some discrepancies, which have been pointed out, appear in certain altitude ranges of the atmosphere. The reason for these differences is not yet clear and could be attributed to an inadequate representation of the vertical transport, to errors in the values of the chemical and photochemical parameters and/or to missing chemistry. These unresolved problems introduce some uncertainties in the quantitative predictions of future ozone and temperature changes provided by the current models used for these predictions.

### 3. RESPONSE OF THE ATMOSPHERE TO PRESCRIBED PERTURBATIONS

#### 3.1 Steady-state calculations

In order to understand the physical and chemical processes involved in the response of the climatic system to chemical emissions in the atmosphere, single perturbations of each trace gas in isolation will first be considered. The variation in the surface temperature resulting from the increase in the amount of greenhouse gases and obtained by a pure radiative model is compared in Table 3 to similar calculations in which the concentration of all species is allowed to vary as a result of chemical and photochemical reactions. The first case is referred to as a pure radiative model and the second as a calculation including chemical feedbacks. Differences are significant for some perturbation gases which significantly influence ozone such as methane and the

chlorofluorocarbons. The inclusion of a detailed chemical code in radiative convective model appears thus to be important for studying the climatic impact of some trace gases. Owens et al. (1985) have also estimated the effect of chemical feedback on the calculated changes of surface temperature. Their study, consistently with ours, suggest very little change for the CO<sub>2</sub> perturbation case and show that the surface warming due to CH<sub>4</sub> is amplified when chemical feedback is included. However, at variance with the present study, the calculations by Owens et al. indicate that the warming due to increasing concentrations of CFCs is somewhat larger when chemical feedback is included. The results reported in Table 3 are however generally in good agreement with other model calculations. For example, for a doubling in CO<sub>2</sub>, the temperature increase derived by Donner and Ramanathan (1980), Lacis et al. (1981), Owens et al. (1985) and Wang and Molnar (1985) is (no chemical feedback) 2.0 K, 2.9 K, 1.67 K and 1.49-2.67 K (depending on the model assumption) respectively. The same studies suggest a temperature increase of 0.30 K, 0.26 K, 0.23 K and 0.26-0.44 K respectively for a doubling of methane and 0.33 K, 0.65 K, 0.29 K and 0.39-0.66 K for a doubling of nitrous oxide.

The potential impact on the stratosphere of individual gases considered in the present study is now estimated by calculating the steady-state ozone and temperature changes for single perturbations by each of these gases using the fully coupled radiative chemical model. For a doubling of CO<sub>2</sub>, a +1.8% and a +15% increase are found for the ozone column and for the ozone concentration

**Table 3**  
**Temperature changes (K) at the surface for**  
**different perturbations**

Perturbation	No chemical feedback	With chemical feedback
CO <sub>2</sub> × 2.0	2.07	1.99
CH <sub>4</sub> × 2.0	0.24	0.38
N <sub>2</sub> O × 1.2	0.06	0.06
CFC × 7.5	0.60	0.40
combined	2.91	2.71
N <sub>2</sub> O × 2.0	0.37	0.27

at 40 km altitude, respectively. The variation in the temperature is -8K at 40 km. For a doubling of the methane content, the corresponding ozone and temperature changes are +2.35%, +5.5% and +0.5K. A 20% increase, predicted for the concentration of tropospheric ozone, could be considerably higher in regions where large amounts of anthropogenic  $\text{NO}_x$  are present. If the concentration of  $\text{N}_2\text{O}$  is increased by 20%, the ozone column is reduced by 1.4% and the ozone concentration at 40 km by 1.8%. A temperature decrease of about 0.3 K is found at 40 km altitude. When the mixing ratio of F-11 and F-12 is uniformly multiplied by 7.5 (leading to a mixing ratio of active chlorine in the upper stratosphere of 9 ppbv), the reduction of the ozone column is 5% and the decrease of the ozone concentration at 40 km 64.5%. The change in the temperature is -10 K at 40 km. Finally, when all perturbations are considered simultaneously, the ozone depletion (total column) is reduced to 1.1%. The decrease in the concentration of  $\text{O}_3$  at 40 km is 51%. The temperature is found to decrease by 25 K at 40 km altitude. These results, which are summarized in Table 4 are in fairly good agreement with other similar studies made for example by Owens et al. (1985), by Wuebbles (see WMO/NASA, 1986) and by Bruehl (see WMO/NASA, 1986). These studies predict a change of +2.9%, +3.5% and +1.2% respectively for a doubling of the  $\text{CO}_2$  content, +4.3%, 2.9% and 1.4% for a doubling in the methane content and -3.9%, -1.7% and -1.2% for a 20% increase in the amount of nitrous oxide.



**Table 4**  
**Ozone changes (expressed in percent) for different perturbations**

Perturbation	Ozone column	Ozone concentration at 40 km
CO <sub>2</sub> × 2.0	+ 1.82	+ 15.3
CH <sub>4</sub> × 2.0	+ 2.35	+ 5.5
N <sub>2</sub> O × 1.2	- 1.40	- 1.8
CFCs × 7.5	- 5.00	- 64.5
combined	- 1.11	- 50.9

For continuing emissions of chlorofluorocarbons in the atmosphere equal to 309 kT/yr for F-11 and 433 kT/yr for F-12, the reduction in the ozone column (compared to a pre-industrial atmosphere) is estimated to be 5.5% when temperature feedback is omitted in the model calculation and 8.7% when it is included.

### 3.2 Time-dependent calculations

We now deal with the potential changes of the temperature and the ozone concentration in the future based on different scenarios for the release in the atmosphere of the chemical compounds already considered in the previous sections. Future changes in the atmospheric concentration of precursor gases are difficult to predict because of our ignorance in some natural processes involved (e.g., our poor understanding of the reasons for methane increases), the uncertain growth in world population, GNP and energy consumption, unexpected changes in consumer's demand, and uncertainties concerning future regulatory measures for economic growth and environmental protection. Nordhaus and Yohe (1983), for example, have considered uncertainties in the future buildup of atmospheric  $\text{CO}_2$ . From an economic model, in which 10 major variables were randomly modified within a given range of uncertainty, the lowest  $\text{CO}_2$  concentration found in year 2100, after 100 model runs, is 370 ppmv, the highest concentration is 2100 ppmv and the mean concentration 780 ppmv. Large uncertainties are also associated with future emissions of other gases such as F-11

the period 1940-1980, the emissions estimated by Simmonds et al. (1983) are used (lower limit after 1958). For the future, a constant emission rate of 100 kT/yr is adopted after 1980. Indeed, better environmental control of the carbon tetrachloride production as an intermediate for the manufacturing of F-11 and F-12 might be expected. Moreover, the use of this product as a grain fumigant is expected to decline and its use as process solvent is small and unlikely to grow to significant levels (CMA, private communication).

The release in the atmosphere of methyl chloroform was insignificant before 1950. The emission estimated by Prinn et al. (1983) is adopted between 1950 and 1976. Then a linear variation is applied to reach 500 kT in 1980. Future trends in the release of this chemical compound are difficult to estimate. The production of methyl chloroform grew rapidly in the 1970's when it was increasingly used to replace other chlorinated solvents. According to recent economic studies (CEFIC, 1985), the market has remained static since 1979 (see also WMO/NASA, 1986). Therefore the release of this gas has been assumed to remain constant for the purpose of the present calculation. This is in contrast to a previous study by Brasseur et al. (1985), in which a substantial increase in the future production of  $\text{CH}_3\text{CCl}_3$  was assumed. This work however indicated that this assumption had only limited effects on the calculated ozone changes.

The emissions of all chlorofluorocarbons used in the model before year 1984 are the same in the first 14 scenarios (1 to 7). For F-11, emissions of 0.0, 0.1, and 0.2 kT/yr are adopted for the period 1910-1938, 1938-1943, and

and F-12, as shown, for example by the recent economic study of Quinn et al. (1986).

The uncertainties associated with future trends in the emission of precursor gases are probably the largest uncertainties in the prediction of future ozone and temperature variations. Therefore, the scenarios used in the present study are not intended to be the most realistic possible but, especially in the case of  $\text{CO}_2$ ,  $\text{CH}_4$  and  $\text{N}_2\text{O}$ , are based on extrapolations of past and present growths. For the chlorofluorocarbons, different scenarios will be considered in order to estimate the impact on the ozone abundance of possible regulatory measures dealing with the production of chlorofluorocarbons.

#### *Adopted scenarios for the time-dependent model simulations*

The numerical simulation of the atmospheric behavior is started in year 1910. The results however are represented only after 1940 and are expressed relative to the values of this particular year. Through this procedure, the small transient effects appearing during the first steps of integration, as a result of the choice of the initial conditions (which are not necessarily in mutual equilibrium), will not affect the results presented in this paper.

Fifteen scenarios (Table 5) are considered and used in the model calculations to be discussed hereafter. The first four of them (1, 1', 2 and 2') assume constant levels of  $\text{CO}_2$ ,  $\text{CH}_4$  and  $\text{N}_2\text{O}$ , taken equal to their values in year 1940. Such calculations are not intended to represent a prediction of the future

**Table 5. Scenarios adopted for the future**

Case	Gases other than CFCs	Production of F-11 and F-12			Production of F-113	Temperature feedback
	Mixing Ratio	Rate %/yr	Capacity Cap	Aerosol Ban	Rate %/yr	
1	constant	3	no	no	not included	yes
1'	constant	3	no	no	not included	no
2	constant	3	yes(1.5) <sup>1</sup>	no	not included	yes
2'	constant	3	yes(1.5)	no	not included	no
3a	increases	0	-	no	not included	yes
3b	increases	0	-	no	3	yes
3c	increases	0	-	no	6	yes
3d	increases	0	-	no	0	yes
4	increases	3	no	yes	6	yes
5a	increases	3	yes(1.5)	no	not included	yes
5b	increases	3	yes(1.5)	no	3	yes
5c	increases	3	yes(1.5)	no	6	yes
6	increases	3	yes(1.5)	yes	6	yes
7	increases	3	yes(2.0)	no	6	yes
8	increases	not incl.	-	-	not included	yes

CH<sub>3</sub>CCl<sub>3</sub> and CCl<sub>4</sub> have constant emission except in scenario 8 where they are not included.

(1.5) means that the capacity cap is 1.5 the production in 1984.

behavior of the atmosphere but are nevertheless performed to isolate the effect of the CICs. In other words, the numerical results obtained for these conditions should not be associated with the future of the real world.

In the remaining scenarios (3a to 8), all greenhouse gases are allowed to vary. The variation as a function of time in the concentration of these gases (except the CICs) is based essentially on the reference set of scenarios suggested by Wuebbles et al. (1984). For carbon dioxide, the historical mixing ratio  $X(t)$  is expressed by the analytical expressions (if  $t$  is the current year)

$$X(t)=270\exp[0.00141(t-1850)]\text{ppmv} \quad (8)$$

for the period between 1910 and 1957 and

$$X(t)=270+44.4\exp[0.019(t-1958)]\text{ppmv} \quad (9)$$

between 1957 and 1983. After 1983, the following extrapolation is adopted:

$$X(t)=341.4+1.539(t-1983)\exp[0.009173(t-1983)]\text{ppmv}. \quad (10)$$

With this projection based on a study by Edmonds et al. (1984), the  $\text{CO}_2$  mixing ratio reaches 600 ppmv in year 2062. In the case of methane, the past mixing ratio is expressed by

$$X(t)=1.0+0.65\exp[0.035(t-1980)]\text{ppmv} \quad (11)$$

for the period 1910-1983. As the cause of the past increase in the methane concentration is not understood and since it is not obvious that the present trend

will remain identical in the future, it is difficult to specify for this gas whose lifetime is of the order of 10 years a plausible scenario for the next hundred years. Therefore, the present growth has been extrapolated after 1983. It should be remembered that this assumption introduces a severe limitation in the ozone and temperature predictions. The historical mixing ratio of nitrous oxide since 1910 is represented by

$$X(t)=285+14\exp[0.04(t-1978)]\text{ppbv.} \quad (12)$$

An increase of 0.25 %/yr is assumed after 1983. Shown in Figure 8 is the evolution of the mixing ratio of CO<sub>2</sub>, CH<sub>4</sub> and N<sub>2</sub>O between years 1940 and 2100.

The chlorocarbons CCl<sub>4</sub> and CH<sub>3</sub>CCl<sub>3</sub> are assumed to vary with the same rate in all scenarios involved in the present study except scenario 8. The emissions in the atmosphere of carbon tetrachloride (expressed in kT/yr) are assumed, according to Wuebbles et al. (1984), to be the following between 1910 and 1932

$$E(t)=0.96\exp[0.388(t-1911)] \quad (1911-1916) \quad (13a)$$

$$E(t)=6.67\exp[0.132(t-1916)] \quad (1916-1922) \quad (13b)$$

$$E(t)=16.0 \quad (1922-1925) \quad (13c)$$

$$E(t)=17.1\exp[0.1067(t-1925)] \quad (1925-1932) \quad (13d)$$

Between 1932 and 1940, a constant release of 44.1 kT/yr is selected, while for

1943-1945 respectively, according to Wuebbles et al. (1984). Between 1945 and 1984, the emissions derived from the production suggested by the Chemical Manufacturers Association (CMA, 1985) are used. Emission of F-12 starts in 1931 with a rate of 0.1 kT/yr, reaching 0.4 kT/yr in 1935, and remains constant until 1940 (Wuebbles et al., 1984). After this period and until 1984, the historical releases derived from CMA production data are adopted. For F-113, the emission starts in 1960 and is based on an estimate of 140 kT/yr in 1984 (WMO/NASA, 1986). It should be noted that the effect of F-113 is not included in all model cases, as will be explained below.

The emissions of the chlorofluorocarbons introduced in the model for a simulation of the potential atmospheric response after year 1984 may differ greatly from one case to another. They are deduced from the following assumptions on the annual production of these compounds. In cases 3a to 3d, the industrial production of F-11 and F-12 is assumed to remain constant and equal to its level of 1984. In cases 1 to 2' and 4 to 7, the productions of F-11 and F-12 increase by 3%/yr after 1984 with a delay however for cases 4 and 6, resulting from a ban on the use of CFCs as aerosol propellants, assumed to have occurred starting in year 1985. This last assumption is supposed to account for a possible generalization of the regulations taken in the United States and several other countries. Moreover, a production cap equal to 1.5 times the production of 1984 is prescribed in cases 2, 2', 5, 5a, 5b, 5c and 6. In case 7, the capacity cap is equal to 2 times the 1984 production. The annual growth rate



of 3% has been arbitrarily selected but is similar to rates adopted in other studies (WMO/NASA, 1986). An increase in the release of F-113 is considered in cases 3b, 3c, 4, 5b, 5c, 6 and 7. Use of F-113 is thought to be growing fairly quickly at present, as a result of its use in current electronics technology (essentially as a solvent to clean electronic assemblies and components). A growth in the production of 6%/yr is therefore adopted after 1984 in cases 3c, 4, 5c, 6 and 7. However, because there is doubt if this growth rate will be maintained in the longer term, an arbitrary growth rate of 3%/yr has been considered in cases 3b and 5b. In all cases, the emission of F-113 (expressed in mass) is never allowed to exceed that of F-11. A constant F-113 production at the 1984 level is assumed in case 3d. Cases 1 to 3a and 5a do not include F-113. Figures 9a and b show the different emission rates adopted for the chlorofluorocarbons after 1940. Numerical values associated with these curves are given in Tables 6a-d.

In most cases, the temperature feedback is included in the model calculations. However, in order to assess the importance of the temperature coupling on the ozone response, the "CIC alone" scenarios have been run assuming either fixed temperature during the model integration (cases 1' and 2') or full radiative coupling including temperature feedback (cases 1 and 2).

### *Atmospheric response*

The ozone and temperature changes calculated in response to the scenarios presented earlier will now be discussed. But, in order to be able to compare the

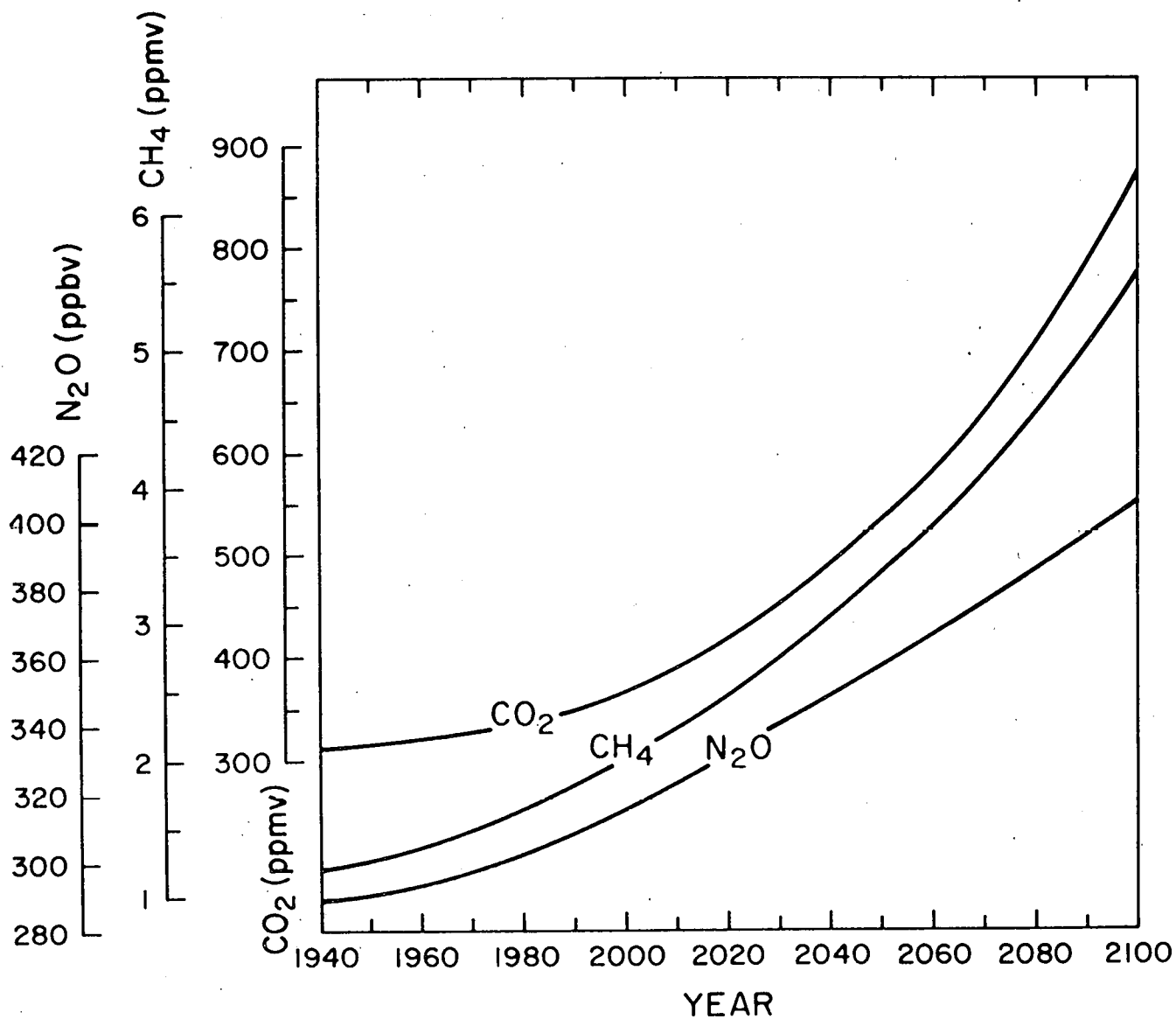


Fig. 8.- Variation in the mixing ratio of CO<sub>2</sub>, tropospheric CH<sub>4</sub> and tropospheric N<sub>2</sub>O as a function of time (1940-2100), adopted in the time-dependent model calculations.

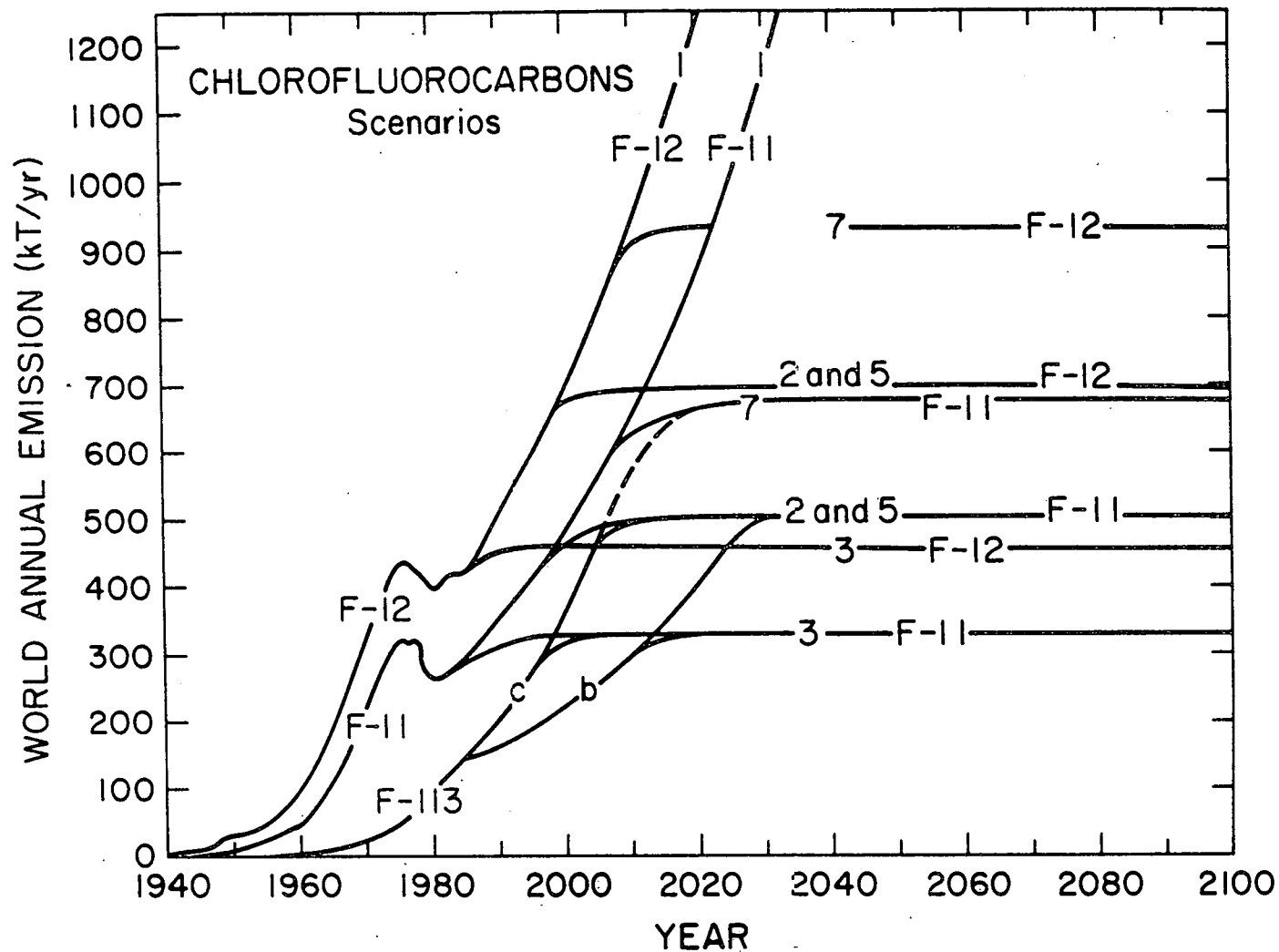


Figure 9a.-Same as Figure 8 but for the world annual emission (kt/yr) of F-11, F-12 and F-13 adopted in different scenarios (1, 2, 3, 5 and 7) listed in Table 5. Note that the emission of F-113 (increase of 3%/yr for case b and 6%/yr for case c) never becomes large than that of F-11.

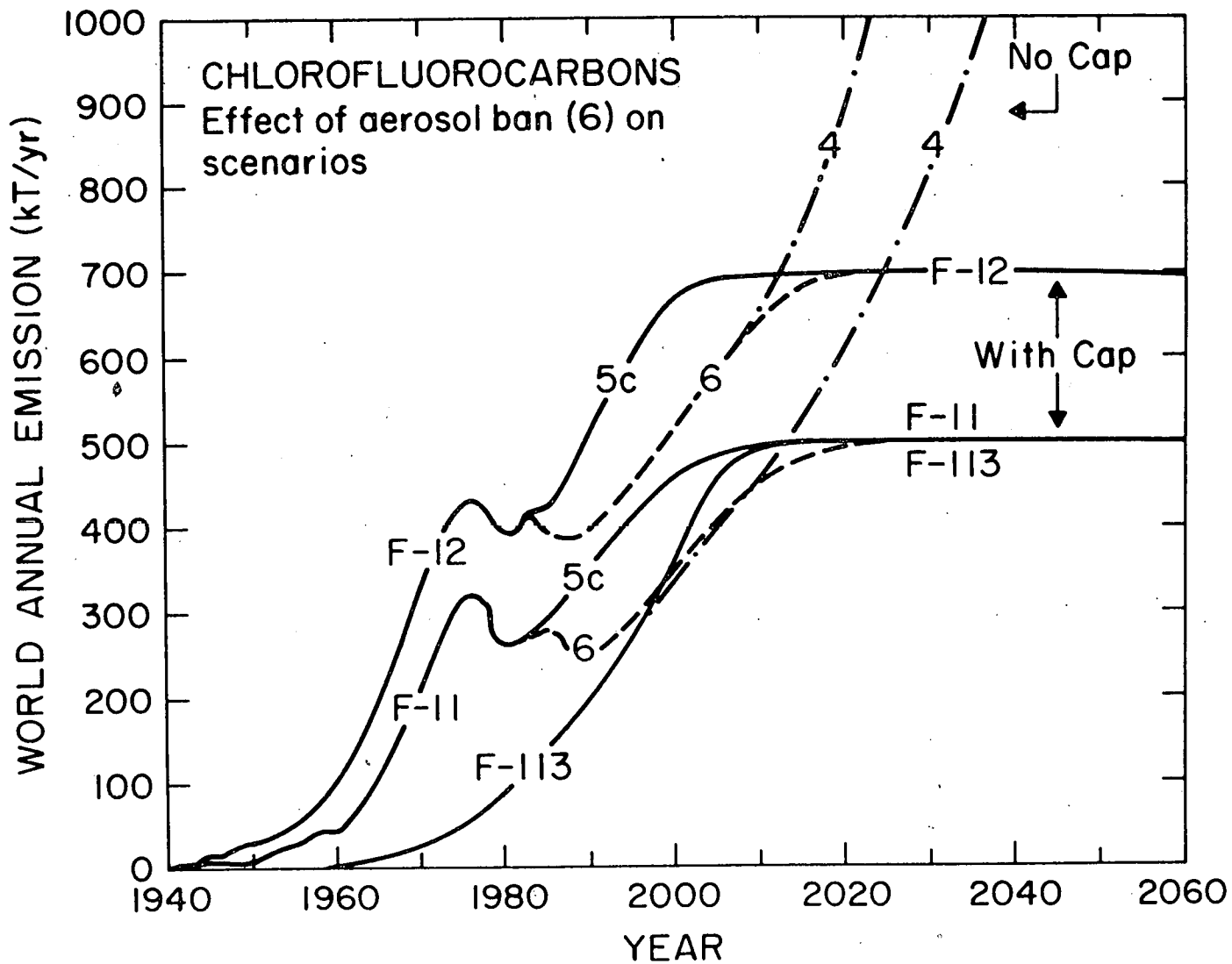


Figure 9b.- Same as Figure 9a but for scenarios 4 and 6 (aerosol ban) compared to case 5c.

**Table 6a**  
**Past emission rates of chlorocarbons (in kT/yr) as a**  
**function of time, adopted in the model calculations**

Year	Scenarios 1 to 7				Scenarios 3b to 4 and 5b to 7
	CH <sub>3</sub> CCl <sub>3</sub>	CCl <sub>4</sub>	F-11	F-12	F-113
1910	0	.96	0	0	0
15	0	6.7	0	0	0
20	0	12.9	0	0	0
25	0	19.0	0	0	0
30	0	32.4	0	0	0
35	0	44.1	0	.4	0
40	0	44.1	.1	.4	0
45	0	69.7	.2	6.4	0
50	0	56.0	5.3	25.7	0
55	8.0	40.7	22.9	47.4	0
60	36.1	39.7	40.6	91.2	2.5
65	72.9	72.4	109.2	181.1	6.5
70	154.5	156.3	209.2	314.7	17.0
75	364.2	100.1	318.3	435.1	44.3
80	481.0	97.2	262.6	388.1	97.3

**Table 6b**  
**Future emissions of F-11 (kT/yr) adopted for the different scenarios**

<b>Year</b>	<b>Scenarios</b>					
	<b>1, 1'</b>	<b>2, 2', 5</b>	<b>3</b>	<b>4</b>	<b>6</b>	<b>7</b>
1985	294.0	294.0	290.5	279.5	279.5	294.0
1990	350.1	350.1	308.3	253.5	253.5	350.1
1995	414.0	414.0	321.6	298.0	298.0	414.0
2000	471.1	471.1	331.2	347.7	347.7	471.1
2010	634.3	497.6	332.9	455.8	455.8	634.3
2020	856.3	503.6	332.9	615.3	494.9	668.7
2030	1156.0	503.6	332.9	830.5	505.5	676.8
2040	1560.6	503.6	332.9	1121.1	505.5	676.8
2050	2106.8	503.6	332.9	1513.3	505.5	676.8
2060	2844.2	503.6	332.9	2042.8	505.5	676.8
2070	3839.7	503.6	332.9	2757.4	505.5	676.8
2080	5183.5	503.6	332.9	3722.1	505.5	676.8
2090	6997.8	503.6	332.9	5024.4	505.5	676.8
2100	9447.1	503.6	332.9	6782.2	505.5	676.8

**Table 6c**  
**Future emissions of F-12 (kT/yr) adopted for the different scenarios**

Year	Scenarios					
	1, 1'	2, 2', 5	3	4	6	7
1985	424.1	424.1	420.4	397.0	397.0	424.1
1990	515.3	515.3	457.0	396.2	396.2	515.3
1995	596.8	596.8	457.4	450.6	450.6	596.8
2000	692.5	676.1	458.2	514.8	514.8	692.5
2010	908.6	693.1	458.2	665.7	665.7	908.6
2020	1226.6	693.1	458.2	898.6	688.6	931.5
2030	1655.9	693.1	458.2	1213.0	688.6	931.5
2040	2235.5	693.1	458.2	1637.4	688.6	931.5
2050	3017.9	693.1	458.2	2210.2	688.6	931.5
2060	4074.2	693.1	458.2	2893.5	688.6	931.5
2070	5500.1	693.1	458.2	4027.3	688.6	931.5
2080	7425.2	693.1	458.2	5436.2	688.6	931.5
2090	10024.0	693.1	458.2	7338.1	688.6	931.5
2100	13532.4	693.1	458.2	9905.4	688.6	931.5

**Table 6d**  
**Future emissions of F-113 (kT/yr) adopted for the different scenarios**

year	3b	3c	3d	4	5b	5c	6	7
1985	144.2	148.4	140.0	148.4	144.2	148.4	148.4	148.4
1990	167.1	198.6	140.0	198.6	167.1	198.6	198.6	198.6
1995	193.8	265.7	140.0	265.7	193.8	265.7	265.7	265.7
2000	224.6	331.2	140.0	347.7	224.6	355.6	347.7	355.6
2010	301.9	332.9	140.0	455.8	301.9	497.6	455.8	561.0
2020	332.9	332.9	140.0	615.3	405.7	503.6	494.9	632.6
2030	332.9	332.9	140.0	830.5	503.6	503.6	505.5	676.8
2040	332.9	332.9	140.0	1121.1	503.6	503.6	505.5	676.8
2050	332.9	332.9	140.0	1513.3	503.6	503.6	505.5	676.8
2060	332.9	332.9	140.0	2042.8	503.6	503.6	505.5	676.8
2070	332.9	332.9	140.0	2757.4	503.6	503.6	505.5	676.8
2080	332.9	332.9	140.0	3722.1	503.6	503.6	505.5	676.8
2090	332.9	332.9	140.0	5024.4	503.6	503.6	505.5	676.8
2100	332.9	332.9	140.0	6782.2	503.6	503.6	505.5	676.8



quantitative effects of the chlorocarbons to other potential perturbations, a model run (scenario 8), in which no ClC (except  $\text{CH}_3\text{Cl}$ ) is included but  $\text{CO}_2$ ,  $\text{CH}_4$  and  $\text{N}_2\text{O}$  are increasing, is first presented. Figure 10 shows the change in total ozone and in the ozone concentration at 1 and 50 km, predicted for this particular case. The calculated change in the ozone column is + 0.88% in 1985, + 1.2% in 2000, + 1.7% in 2020, + 2.3% in 2040, + 3.1% in 2060, + 4.1% in 2080 and + 5.1% in 2100. This increase results from an enhancement in tropospheric ozone (7.3% in 1985, 9.4% in 2000, 14.6% in 2040, 21.5% in 2100 at 1 km) and a decrease in stratospheric ozone (-1.6% in 1985, -2.5% in 2000, -4.1% in 2040, -7.0% in 2100). The increase in tropospheric ozone is actually a result of the growth in methane, while the decline in stratospheric ozone is linked essentially to the increase in nitrous oxide. In this calculation the mixing ratio of  $\text{NO}_x$  is of the order of 50 pptv in the middle troposphere. It should be noted that, since the effect of thermal inertia provided by the global ocean is neglected in the model, the calculated time history of tropospheric ozone shown in Figure 10 (and in Figure 17) might be somewhat approximate, since the surface temperature influences tropospheric water vapor, tropospheric OH, and hence the global tropospheric chemistry. The primary effects influencing future tropospheric ozone changes appear however to be rapid growths in methane and nitrogen oxides.

To determine how rapidly the stratospheric ozone responds to the release in the atmosphere of the ClCs, it should be remembered that the global lifetime

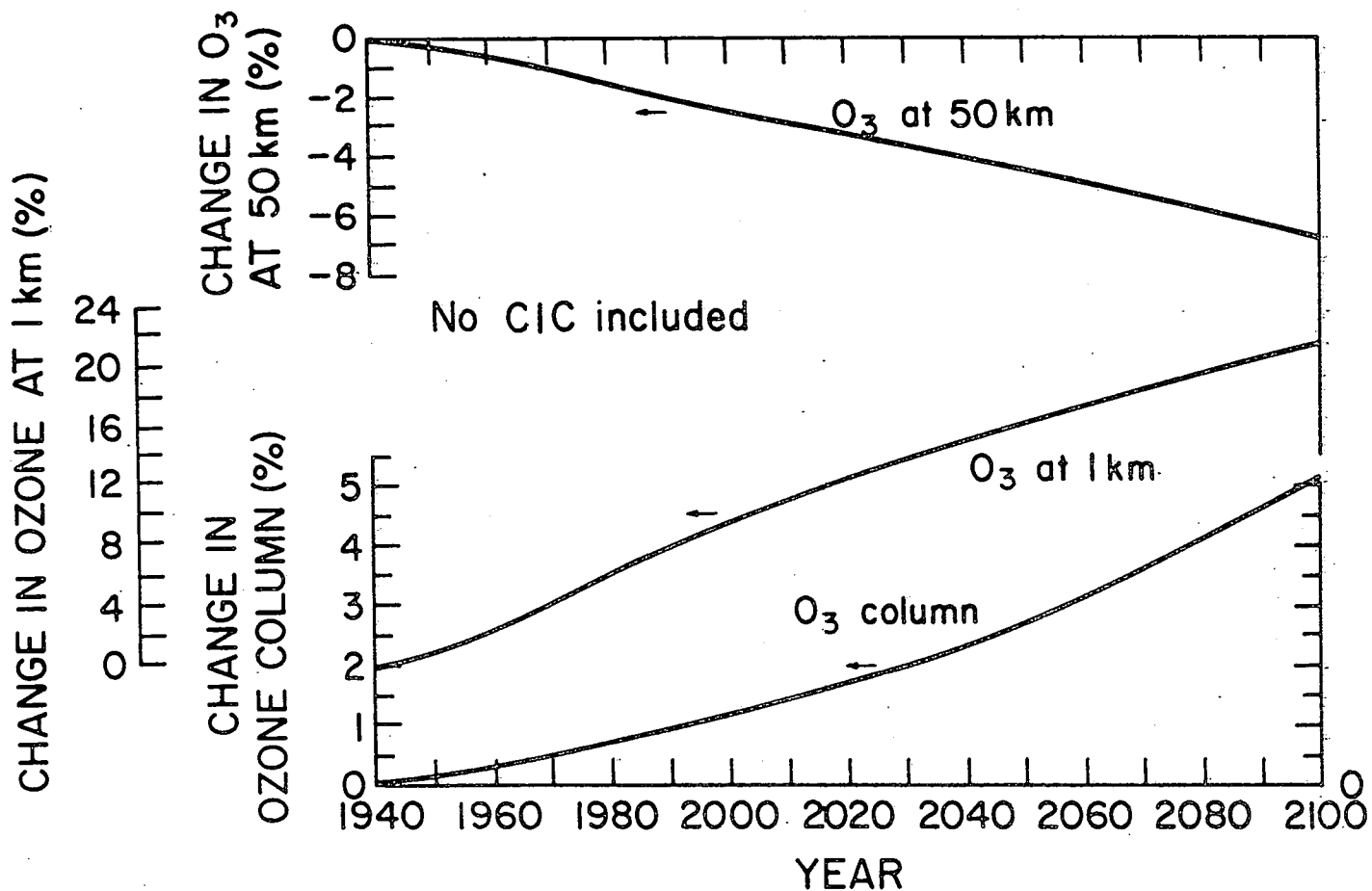


Fig. 10.-Relative variation in the ozone column and in the ozone concentration at 1 and 50 km altitude, calculated as a function of time (1940-2100) for perturbations in  $\text{CO}_2$ ,  $\text{CH}_4$  and  $\text{N}_2\text{O}$  as specified in Figure 8. The impact of man-made chlorocarbons is ignored in this calculation.

of molecules such as F-11 and F-12 is significantly longer than the photochemical lifetime of these molecules in the upper stratosphere where their destruction takes place ( $\sim 1$  year at 30 km) and than the characteristic time associated with vertical transport of these species from their source to their sink region. As shown by Stordal et al. (1985), the long turn-over time for source gases, which are essentially inert in the lower atmosphere, is explained by the large differences in density between the level where they are emitted (surface) and where they are destroyed (30-40 km). When free chlorine atoms are released in the upper stratosphere, essentially by photodecomposition of the ClCs, they react rapidly with ozone, whose chemical lifetime at these heights is of the order of a day. In order to estimate the response time of the atmosphere to ClC perturbations, a time-dependent model run has been performed (with constant amounts of  $\text{CO}_2$ ,  $\text{CH}_4$  and  $\text{N}_2\text{O}$ ). In this run, the emission of the ClCs (except  $\text{CH}_3\text{Cl}$ ) has been arbitrarily put to zero after 1984. The behavior of  $\text{Cl}_x$  and of the ozone column before and after this total ClCs ban is shown in Figure 11. It can be seen that the mixing ratio of  $\text{Cl}_x$  at 50 km continues to increase during approximately 16 yrs and then recovers very slowly. The ozone column continues to decrease during 8 yrs (and not 16 yrs as  $\text{Cl}_x$  below 50 km recovers sooner than at the stratopause). After 1993, the column builds up and reaches the 1985 value in year 2025 and the 1976 value in year 2080.

Attention will now be given to the "ClC alone" cases in order to understand the specific long-term effects of these compounds. Again, these scenarios

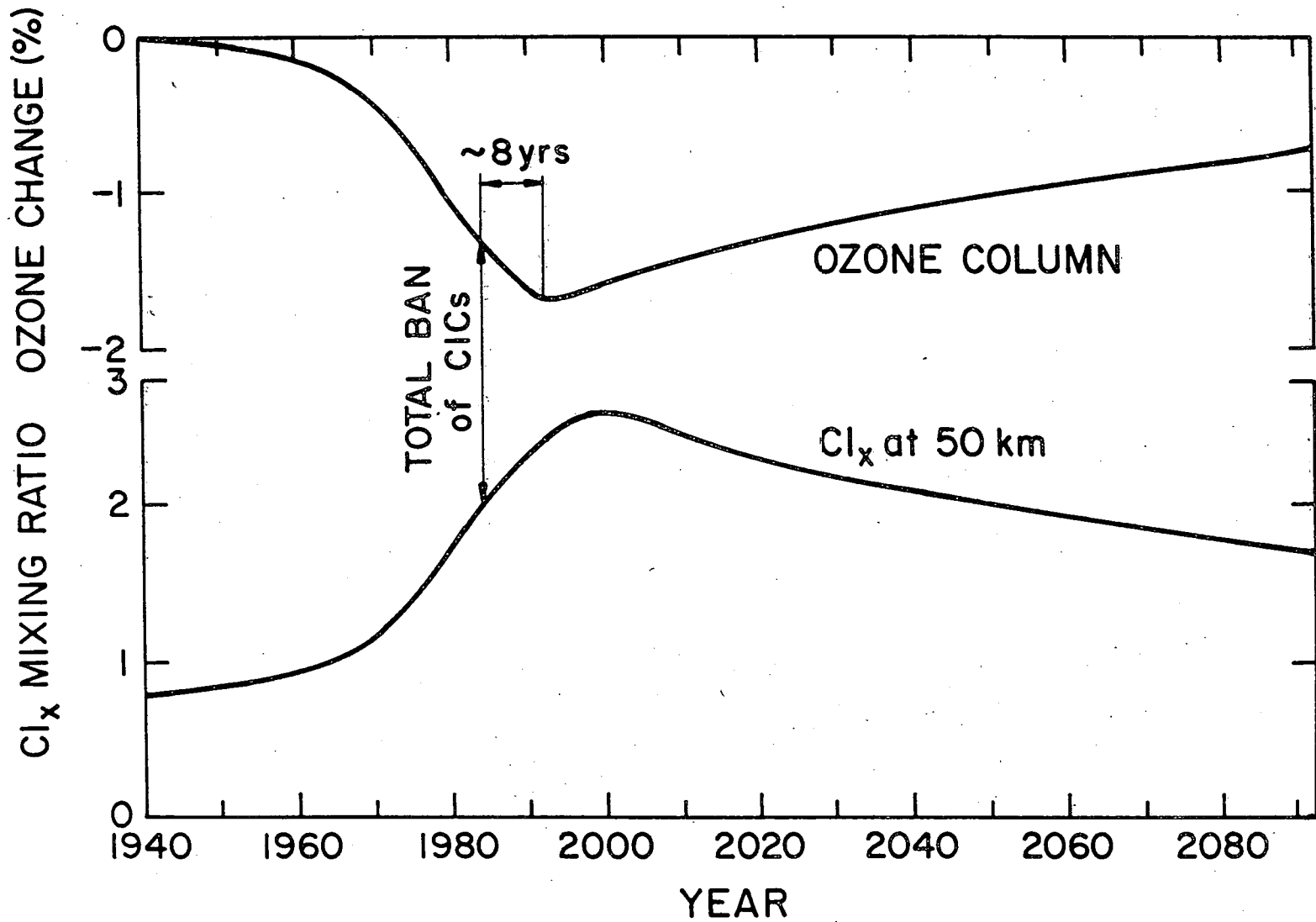


Fig. 11.-Evolution of the Cl<sub>x</sub> mixing ratio at 50 km altitude and of the change in the ozone column if the emission of ClCs are totally stopped in year 1985.

are not intended to simulate the real world as the growth in the chlorocarbons will manifest itself together with the increase of the other trace gases. Shown in Figure 12 is the change in the ozone column derived for the 2 scenarios assuming a fixed temperature (cases 1' and 2') or allowing the temperature to vary (cases 1 and 2). For both scenarios, the response including temperature feedback is larger than if the temperature is not allowed to change. This is fully consistent with the results discussed earlier when steady-state conditions were assumed. If no limitation is imposed on global CFC production (cases 1 and 1') the ozone depletion becomes dramatic especially after year 2040 as it reaches values larger than 20% in 2070 and larger than 30% 8-10 years later. The mixing ratio of total inorganic chlorine in the upper stratosphere reaches 2.8 ppbv in year 2000, 5.2 in 2020, 9.3 in 2040, 16.0 in 2060 and 29.0 in 2080. These latter values are so high that essentially all  $\text{NO}_x$  molecules are titrated by  $\text{Cl}_x$ , so that a strong non-linear behavior is predicted by the model. When a capacity cap of 1.5 times the present CFC production level is applied (cases 2 and 2'), the reduction in the ozone column is still significantly reduced (2.5% in 2000, 5.5% in 2040 and 9% in 2100 when the temperature feedback is included). The change appears to be essentially linear with time. Indeed the relative concentration of total chlorine is 2.7 ppbv in year 2000, 4.8 in 2020, 6.8 in 2040, 8.5 in 2060, 10.0 in 2080 and 11.3 in 2100 and thus never exceeds the mixing ratio of total  $\text{NO}_x$ .

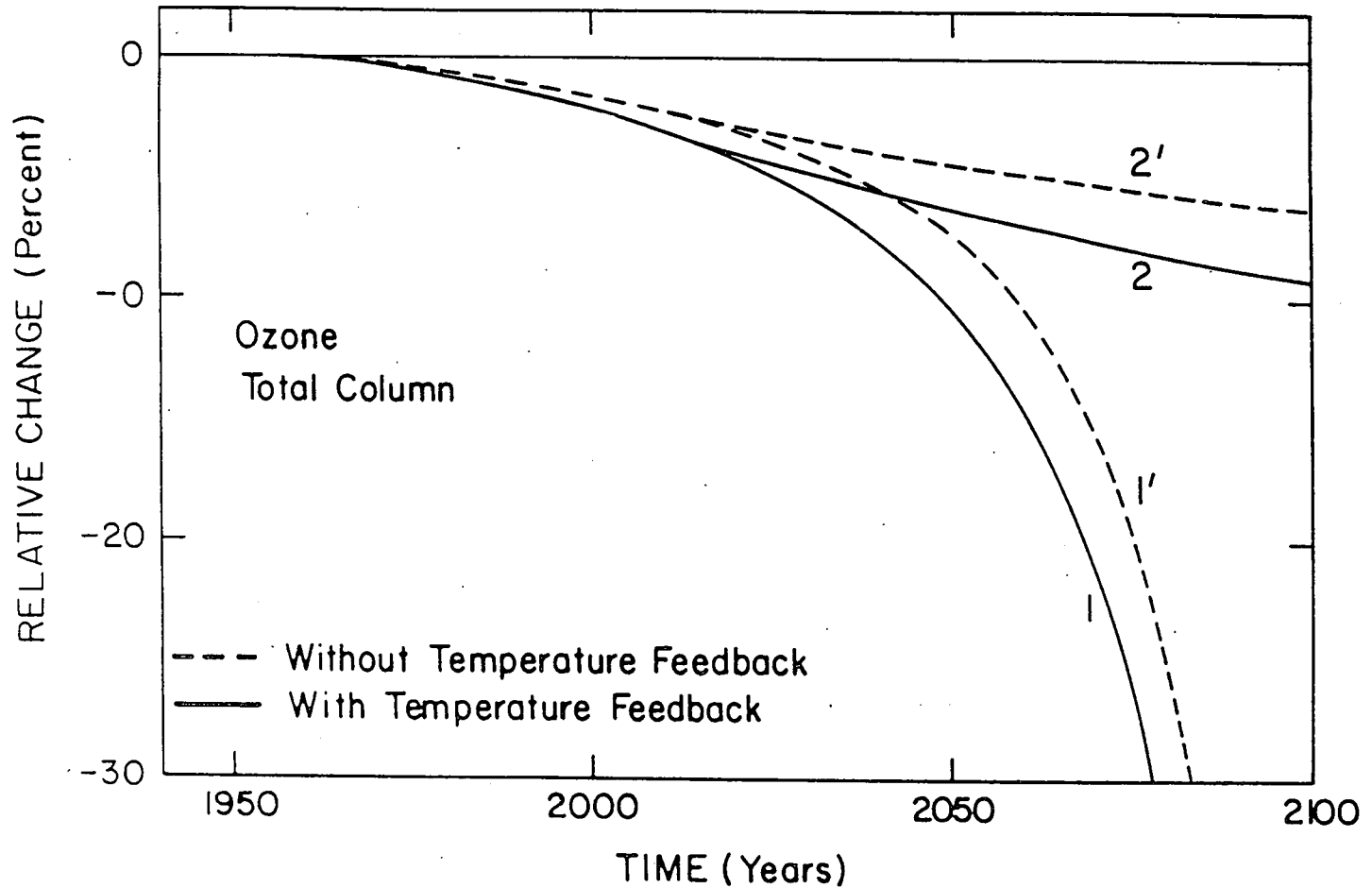


Fig. 12.-Relative change in the ozone column for cases 1 and 1' (increase of 3%/yr in the F-11 and F-12 production rate) and for cases 2 and 2' (production of F-11 and F-12 assumed to remain constant at their 1985 level). The effect of a  $\text{CO}_2$ ,  $\text{CH}_4$  and  $\text{N}_2\text{O}$  increase is not taken into account. Calculation with and without temperature feedback are shown.

We now consider somewhat the more realistic cases (3 to 7) in which all perturbations are involved simultaneously. In these model simulations, the effect of the temperature feedback is fully included. However the change in the chemical composition associated with the variation in the solar ultraviolet irradiance over an 11-year solar cycle is not considered. But from the model calculations of Brasseur et al. (1986) and the analysis of satellite data by Keating et al. (1986), it can be deduced that between solar maximum and solar minimum, the ozone column should be reduced by  $1.7 \pm 1\%$  and the ozone concentration in the upper stratosphere (2 mb) by  $2 \pm 1\%$ . These periodic variations have to be superimposed on the long-term changes associated with the anthropogenic perturbations.

The change in the ozone column for a constant F-11 and F-12 production at the 1984 level, including the effect of the expected  $\text{CO}_2$ ,  $\text{CH}_4$  and  $\text{N}_2\text{O}$  increase is shown in Figure 13a. The different curves correspond to different conditions for the F-113 emission. In all cases, the ozone content increases slightly between 1940 and 1970, as, during this period, the effects of carbon dioxide and methane largely compensate the action of the CFCs and of nitrous oxide. The increase, however, is never larger than 0.1% and is thus too small to have been detected. After 1970, the ozone starts to be depleted essentially by anthropogenic chlorine. The rate of decrease is for example larger in case 3c than 3a, showing the long-term effect of F-113. After year 2040 in case 3a and 2060 in case 3c, the ozone column starts to increase again as a result of the fast

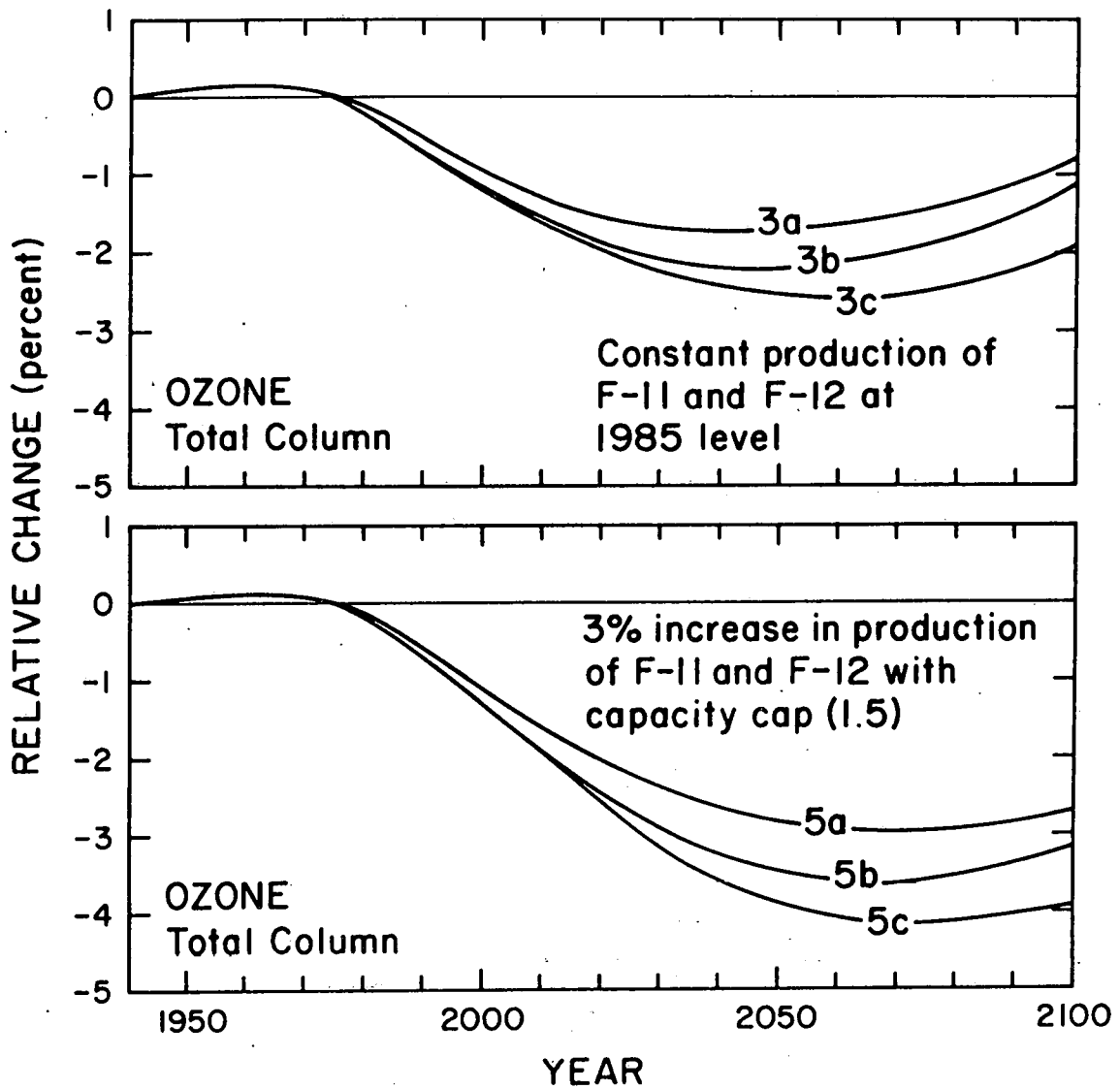


Fig. 13.-Relative change in the ozone column (a) for cases 3a-c and (b) for cases 5a-c between 1940 and 2100. The effect of a simultaneous increase in  $\text{CO}_2$ ,  $\text{CH}_4$  and  $\text{N}_2\text{O}$  (Figure 8) is taken into account.



growth in methane. This effect will be discussed in more detail when the altitude dependence of the ozone response will be considered. Similar cases, but for a 3%/yr increase in the F-11 and F-12 production, with a capacity cap of 1.5 times the 1984 production level, are shown in Figure 13b. As in the previous cases, after a small increase before 1970, the ozone column starts to decrease to reach for case 5a a maximum reduction of 2.8% in 2070 and for case 5c a maximum reduction of 4.2% in 2080. Thereafter, a slow increase takes place.

Different measures have been suggested to regulate the production or the use of the chlorofluorocarbons. We now consider the impact of two possible regulatory measures: (1) the adoption of a cap below which the world production capacity of the CFCs must remain; the sensitivity of the ozone column to the level of this cap will be considered, (2) an immediate total ban of the CFCs as propellant agents in aerosol cans. For brevity this latter case will be referred as "aerosol ban."

The ozone response, calculated for two different levels of the capacity cap (1.5 times the 1984 production--case 5c--and 2.0 times this level--case 7-- ) is shown in Figure 14. In both cases, the increase of the F-11 and F-12 production, after 1984 and before the capacity cap is reached, is assumed to be 3%/yr. The emission rate of F-113 increases by 6%/yr until it reaches the emission level of F-11 and remains constant thereafter. In both cases, the ozone depletion is significantly lower than when no cap is applied. Furthermore, the maximum ozone depletion, which is 4.2% when a capacity cap of 1.5 is adopted,

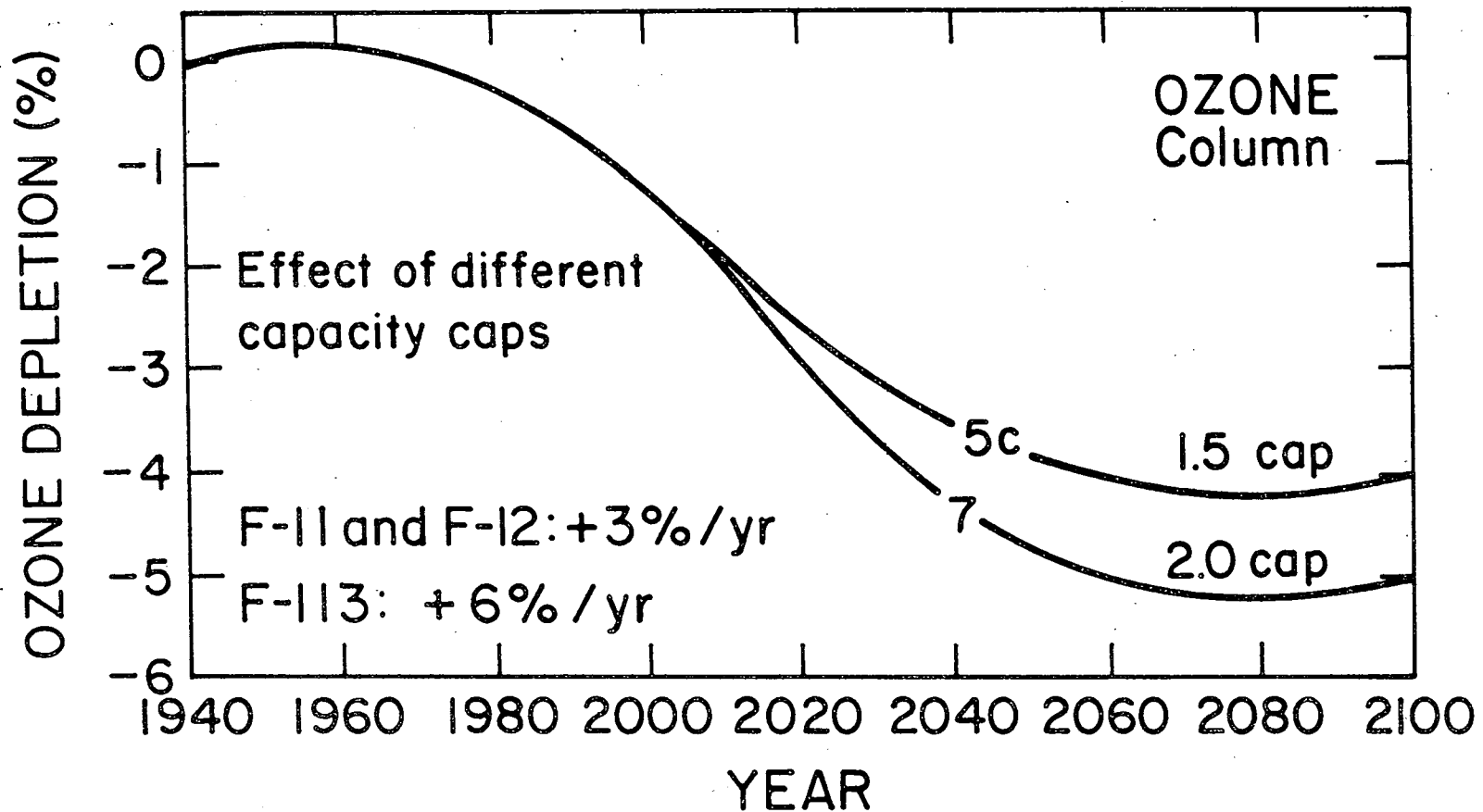


Fig. 14.-Effect of different capacity caps (1.5 and 2.0 the present production level of F-11 and F-12) on the change in the ozone column between years 1940 and 2100.

becomes 5.2% when this cap equals 2 times the 1984 production level.

If the future 3% increase in F-11 and F-12 is delayed by an aerosol ban and if no capacity cap is applied, the ozone depletion is also delayed but finally reaches dramatic levels. Figure 15a indicates that, in a case similar to 5c but with an aerosol ban and no capacity cap (case 4), the ozone reduction (referred to the 1940 value) is less than 1% before 1990 and less than 2% before 2015, but reaches 10% in 2060 and 30% in 2080. Finally, the case referring to an aerosol ban with capacity cap (case 6) is compared in Figure 15b to a similar case (5c) with the same capacity cap but no aerosol ban. It clearly appears that the difference between the two model predictions is small (less than 0.5%) until 2055. In 2100, the difference is less than 1%.

In order to estimate the possible model dependence of these results, model simulations with scenarios 3c and 5c have also been performed with the radiative code C2. Again, it should be remembered that this code is conceptually different from code C1, although both of them provide results for the present-day atmosphere which are in fairly good agreement with the observation. The calculated change in the ozone column for the two models and the two perturbation cases is shown in Figure 16. Obviously, model C1 (which is used in most of this paper) leads to larger ozone reductions. For example, in case 5c, the maximum ozone reduction is 4.2 % when model C1 is used and 1.8% only with model C2. This has, at least in part, to be attributed to the difference in the temperature change calculated by the 2 models in the region where most of the

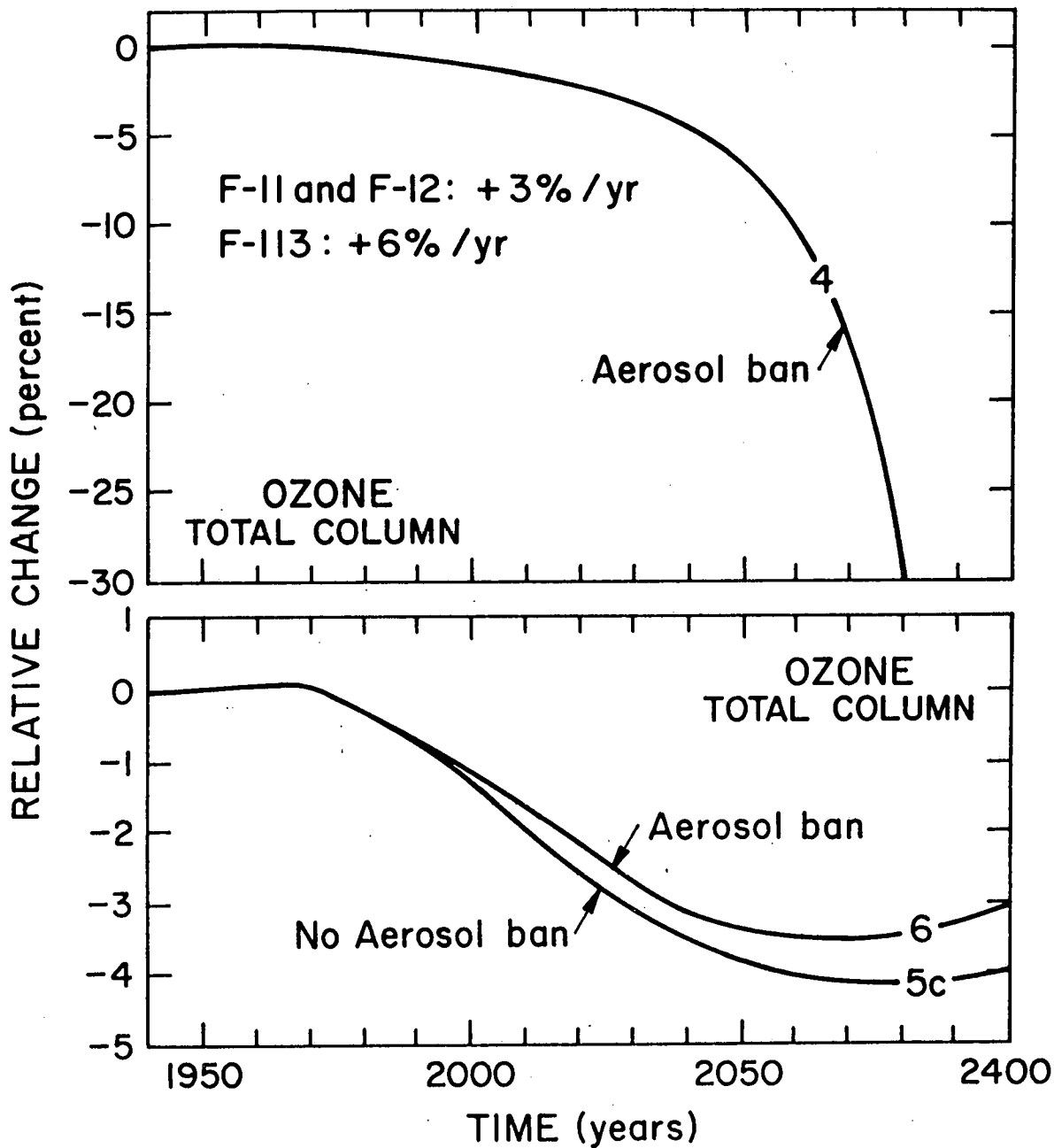


Fig. 15.-Effect of a ban in the use of F-11 and F-12 as aerosol cans propellants on the change in the ozone column (a) without capacity cap - case 4; (b) with capacity cap - case 6 compared to case 5c.

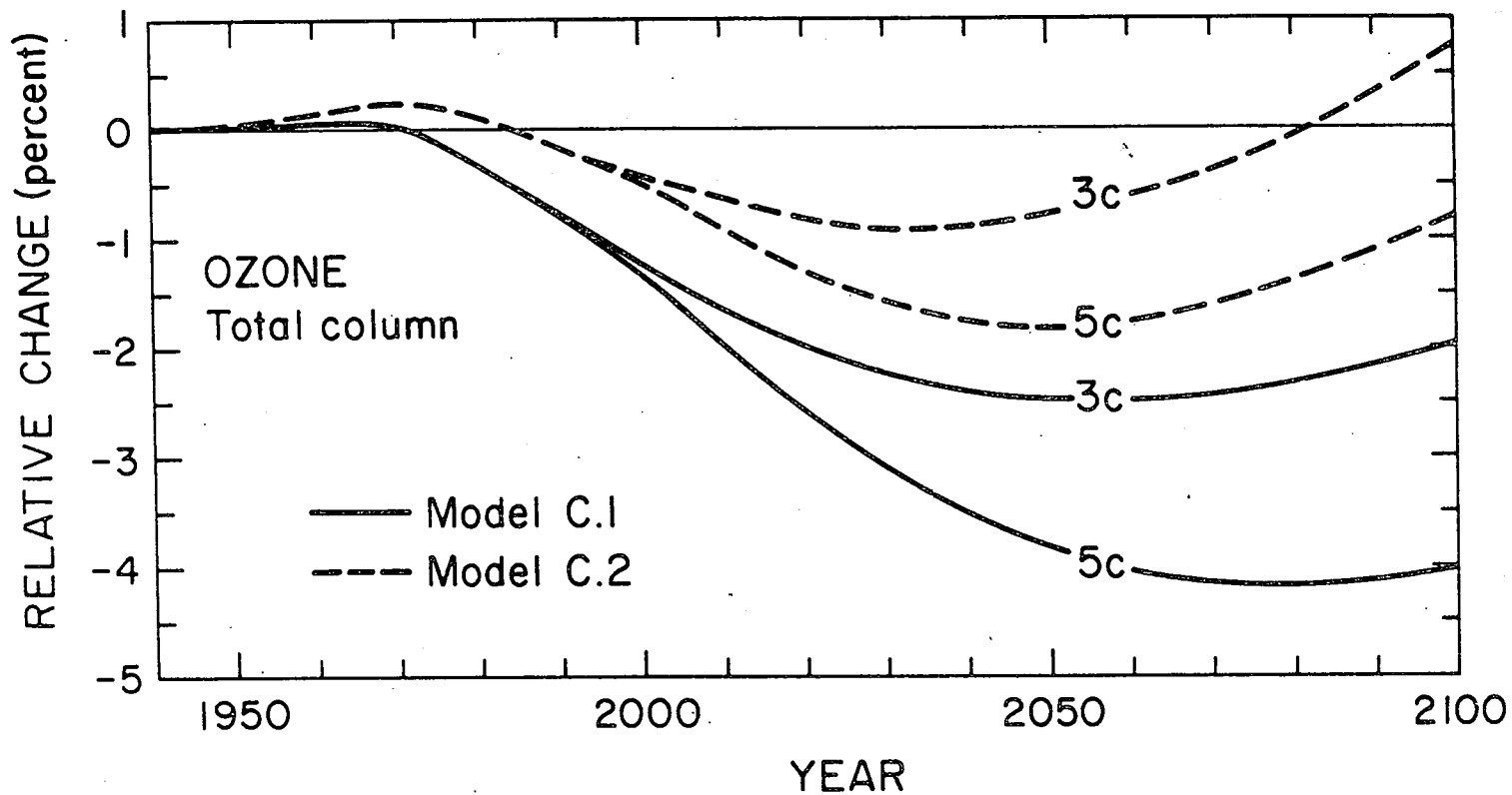


Fig. 16.-Comparison between changes in the ozone column for scenarios 3c (constant production in CFCs at the 1985 level) and 5c (3% increase in the CFCs production with a capacity cap at 1.5 times the 1985 level) obtained with radiative codes C1 and C2, respectively.

ozone is confined and where, despite the fact that the chemical lifetime of ozone becomes larger than the dynamical lifetime, the sensitivity of the ozone chemistry to the temperature changes is still significant. Such a comparison of 2 models, in which the chemistry is entirely identical, clearly shows that differences in the results obtained by the several models used for example in the WMO/NASA intercomparison are not surprising.

The change in the ozone column, which has been previously discussed, is an important parameter to assess the expected variation in the ultraviolet irradiance at the earth's surface and the related biological consequences. The determination of the changes in local ozone is also important since the heating rate and consequently the temperature depend not only on the transmission of solar UV radiation in the atmosphere but also on the ozone concentration as a function of altitude. Changes in ozone, especially in the stratosphere, and related variations in the temperature may cause significant modifications in the general circulation of the atmosphere with potential effects in the troposphere. These dynamical feedbacks, as well as their impacts on the earth's climate, are difficult to assess quantitatively. As they require sophisticated three-dimensional models, they will not be considered in the present study.

The effect, as a function of height, of increasing emissions of trace gases will be discussed for one particular case, namely scenario 5c. Figure 17a shows the change in the ozone concentration as a function of height for years 2000, 2040 and 2100, and Figure 17b the same variations but expressed as a function

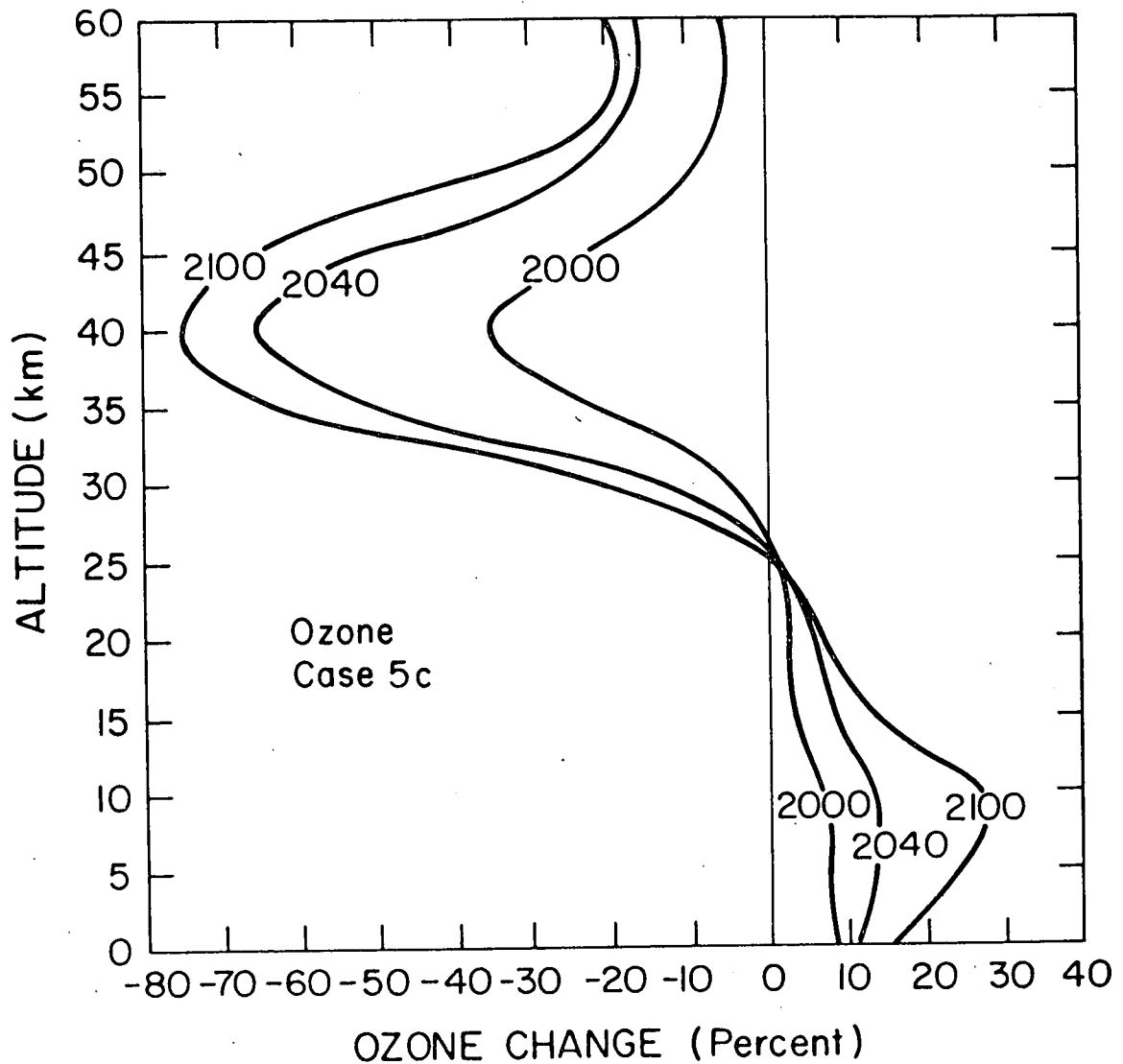


Fig.17a.-Relative variation (percent) of the ozone concentration between 0 and 60 km altitude calculated for years 2000, 2040 and 2100, in the case of scenario 5c (3%/yr increase in F-11 and F-12 with capacity cap at 1.5 times the 1985 production level; 6%/yr increase in F-113 emission with an upper limit equal to the emission of F-11; increase in the concentration of other trace gases - see Fig. 8 -; temperature feedback included).

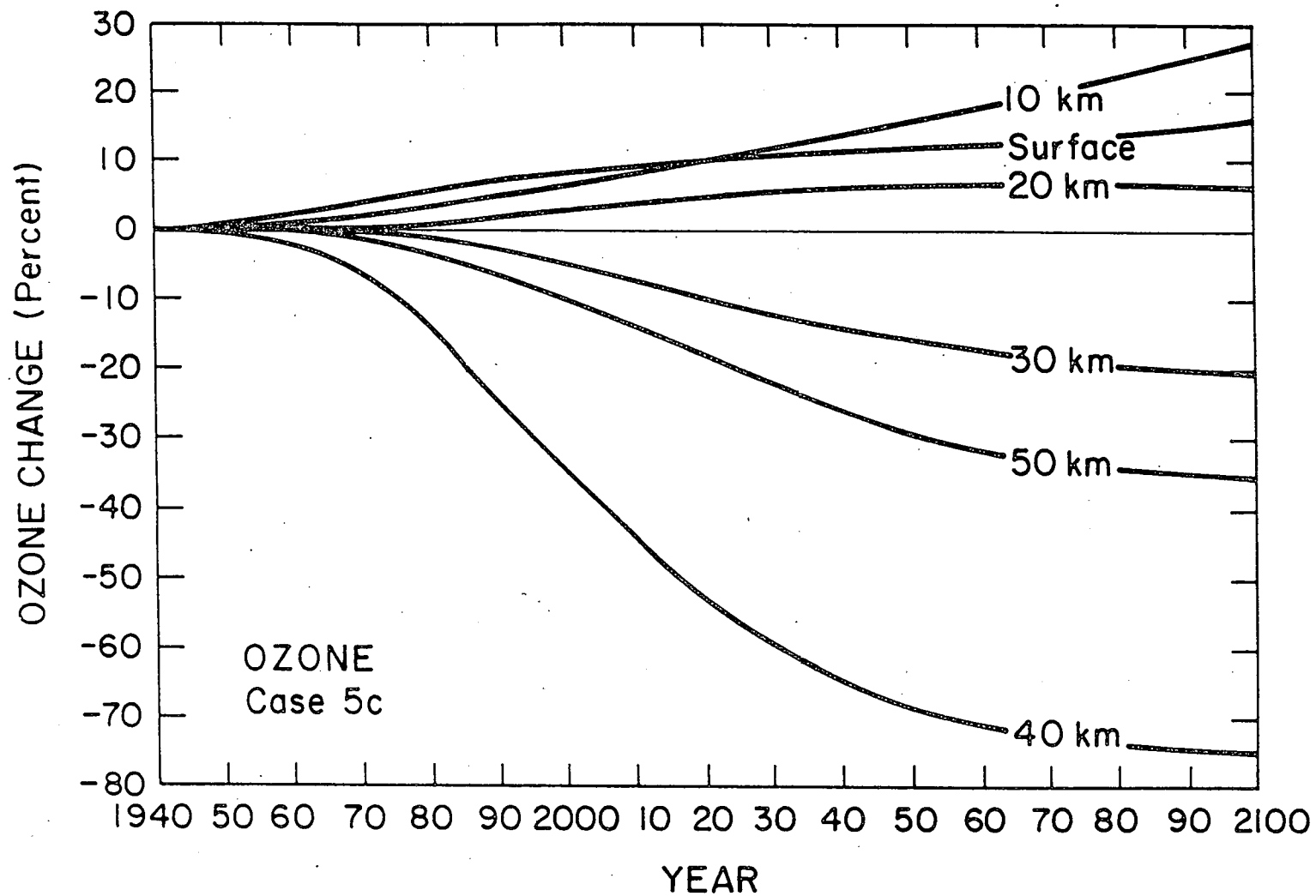


Fig.17b.-Relative variation (percent) as a function of time (1940-2100) of the ozone concentration calculated at selected altitudes for scenario 5c (same conditions as in Fig. 17a).



of time, at selected altitudes from the surface to 50 km. Clearly, ozone is significantly depleted above 25 km with a maximum (for the relative change) at 40 km. The rate of change is rapid after 1990 but decreases after 2020 and tends even to zero around 2100. In fact, during the last part of the integration, the amounts of methane is so high that most chlorine atoms are rapidly converted into HCl. In the lower stratosphere and in the troposphere, ozone increases as a function of time. This behavior results from the self-healing effect of the atmosphere but also, particularly in the troposphere, from the enhanced methane concentration. Indeed, methane in the presence of nitrogen oxides may produce significant amount of ozone below 15 km altitude. According to the model, the increase in the tropospheric O<sub>3</sub> concentration in 1985 compared to 1940 should be of the order of 5%. It could reach on the average 25-30% in year 2100.

The change in the temperature profile is shown in Figure 18 as a function of time for 20, 30, 40 and 50 km altitude. A cooling is predicted above 30 km with a maximum at 45 km. These temperature changes, resulting from the decrease in the ozone concentration and the increase in the amount of carbon dioxide, are sufficiently large to induce significant dynamical perturbations.

#### 4. UNCERTAINTIES IN MODEL CALCULATIONS

The results given previously to characterize the chemical and radiative response of the atmosphere, especially the variation in the total ozone content,

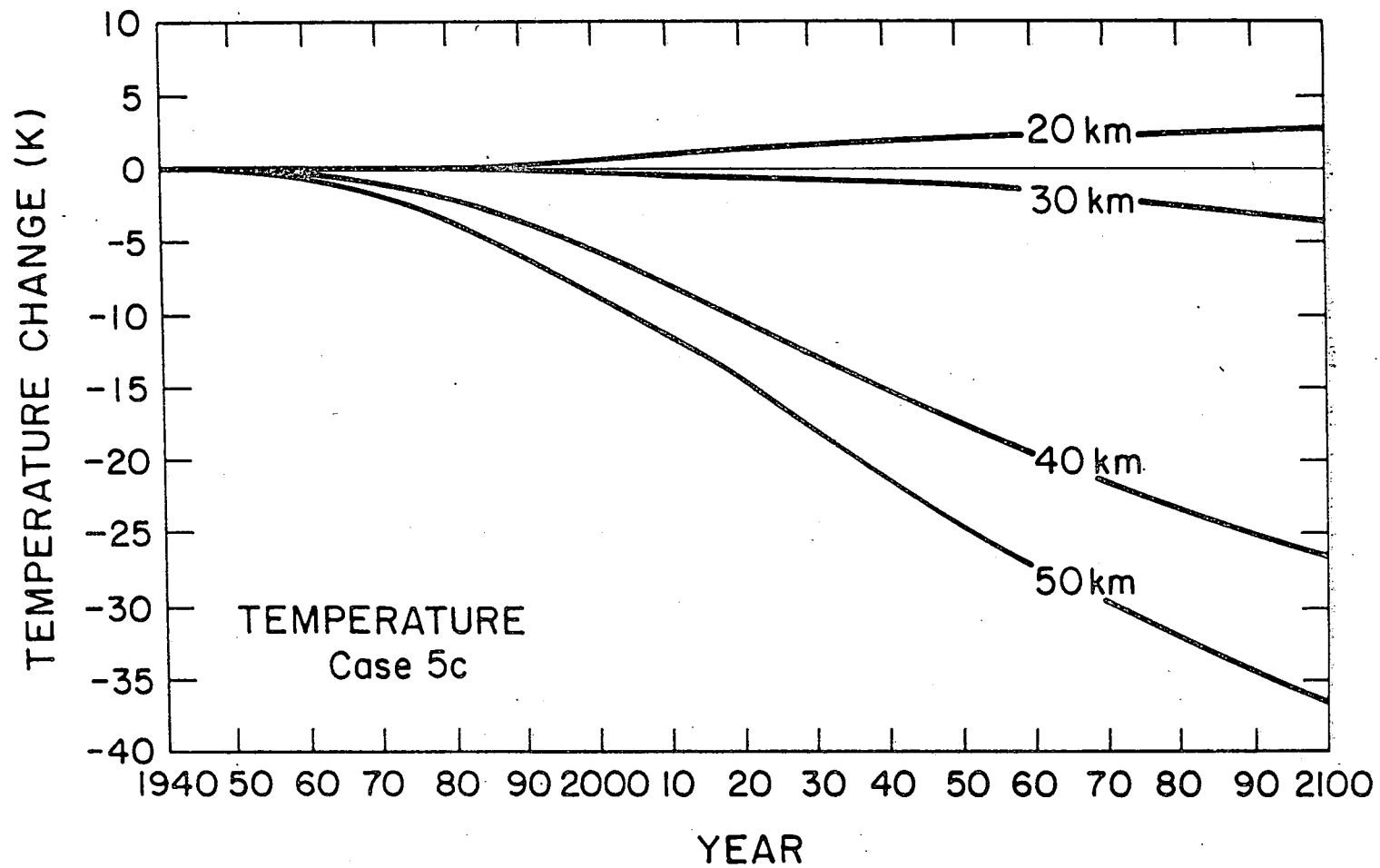


Fig. 18.-Same as Figure 17b but for the variation (Kelvin) in temperature.

are somewhat uncertain. Indeed, the reduction in the ozone column, which is of the order of a few percent, is a difference between 2 large variations in the  $O_3$  concentration: the first of them, located in the upper stratosphere, results from direct chemical actions including significant temperature feedback effects and the second, occurring at lower altitude in the region where most of the ozone is confined, is largely a consequence of the self-healing effect. In other words, the resulting column change is highly dependent on the treatment of the non-linear transmission of solar radiation in the atmosphere. Moreover, as shown by a comparison of the results provided by the 2 radiative codes involved in the present study, the calculated temperature change in the middle and lower stratosphere impacts significantly on the calculated change in the ozone column. It is thus important for 1-D models to treat with some detail the radiative transfer processes, including convective adjustment, all the way down to the surface, instead of using simpler codes in which radiative equilibrium conditions are assumed.

Uncertainties also remain in the chemical scheme which is adopted. For example, 1-D models usually predict a maximum mixing ratio of 13-20 ppbv (WMO/NASA, 1985) for total active nitrogen ( $NO_y$ ) near 35 km, while values inferred from LIMS data (Gille et al., 1984; Russell et al., 1984 and Callis et al., 1985) suggest maximum values larger than 20 ppbv and probably close to 24 ppbv. As seen in Figure 19, the background amount of  $NO_y$  is a crucial parameter for the calculation of the ozone depletion by active chlorine (see also

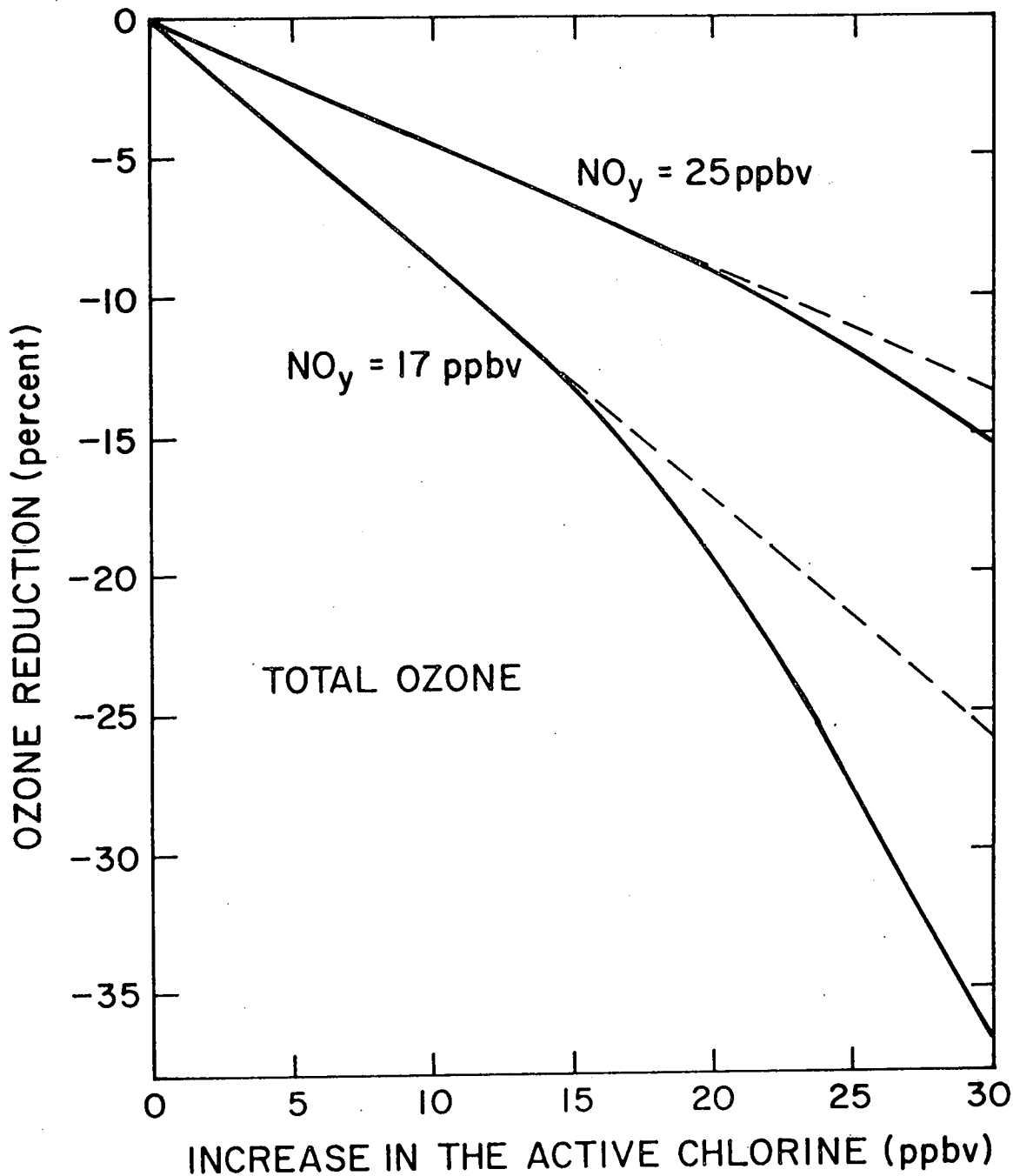


Fig. 19.-Relative change in the ozone column as a function of additional amounts of active chlorine in the atmosphere, for 2 different levels of odd nitrogen. The vertical profiles of  $\text{Cl}_x$  and  $\text{NO}_y$  assumed for this calculation are similar in shape to those shown in Figure 7. The values appearing on this graph refer to the mixing ratio of  $\text{Cl}_x$  at 50 km and of  $\text{NO}_y$  at 35 km.

Brasseur et al., 1985 and Isaksen and Stordal, 1986). Indeed, the sensitivity of ozone to chlorine is reduced by approximately a factor 2 when the  $\text{NO}_y$  mixing ratio is increased from 17 to 25 ppbv. Moreover, the range over which the ozone response is linear with the build up of  $\text{Cl}_x$  becomes wider when the amount of odd nitrogen increases. For an enhancement in the  $\text{Cl}_x$  mixing ratio  $\Delta\text{Cl}_x$  (at 50 km) of less than 15 ppbv (linear regime), and for an  $\text{NO}_y$  relative concentration (at 35 km) between 17 and 25 ppbv, the variation in the ozone column ( $\Delta\text{O}_3$ ) can be expressed by the following numerical expression

$$\Delta\text{O}_3(\%) = \left\{ -1.725 + 0.05[\text{NO}_y] \right\} \Delta\text{Cl}_x \quad (6)$$

where  $[\text{NO}_y]$  and  $\Delta\text{Cl}_x$  are expressed in ppbv. This expression was obtained from an interpolation of the model results for which the amount of other species such as  $\text{CH}_4$ ,  $\text{N}_2\text{O}$  and  $\text{CO}_2$  was kept fixed. Parametric expressions for various conditions including simultaneous increases in the atmosphere content of different gases are given by Connell (1986). As our model calculations probably underestimate the amount of active nitrogen in the atmosphere, the calculated ozone depletions related to increasing emissions of ClCs might represent upper limits. Further consideration should be given to the nitrogen budget in the stratosphere in order to resolve the discrepancy between observed and calculated amounts of  $\text{NO}_y$ .

Uncertainties in the chlorine chemistry are still important. For example, as noted by Brasseur et al. (1985) and more recently by Isaksen and Stordal (1986), the calculated ozone depletion is sensitive to the relative efficiency of both channels in reactions



The reaction scheme recommended by DeMore et al. (1985) does not consider path (b) but, if a probability of occurrence of 15% is assumed according to Burrows et al. (1984), the calculated ozone depletion should be reduced by 25-30%. Additional laboratory work on this problem is urgently required.

Finally, the calculated ozone depletion is significantly affected by the value of the eddy diffusion coefficient which is adopted. The steady-state ozone variation resulting from identical CFC emissions, calculated with the same model input, except for the eddy diffusion coefficient (see Figure 2), is shown in Figure 20. As the vertical transport and lifetime of the source gas are greatly affected by the strength of the average vertical exchanges in the atmosphere, the vertical distribution of these source gases and consequently of the active species is modified together with the K coefficient. The model shows for example that the maximum value of the  $\text{NO}_x$  mixing ratio is increased when vertical exchanges are stronger. This situation arises because the  $\text{N}_2\text{O}$  concentration in the upper stratosphere is enhanced. In contrast, the concentration of active chlorine (Cl,

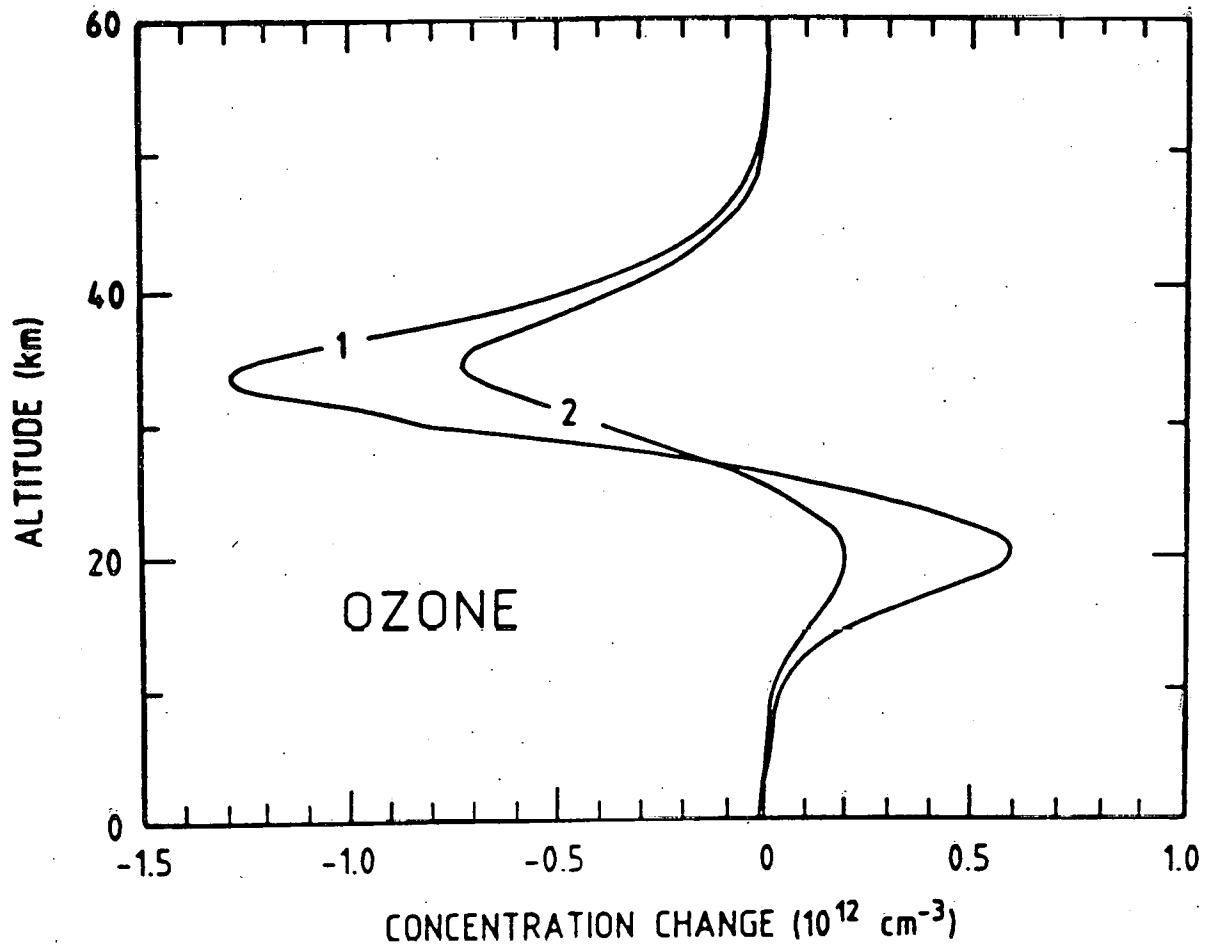


Fig. 20. - Effect of different eddy diffusion profiles (see Figure 2 for the definition of cases 1 and 2) on the ozone change in response to a CFC perturbation.

ClO) in the upper stratosphere and consequently the loss rate of ozone by odd chlorine is reduced as the eddy diffusion coefficient becomes larger. This is a direct consequence of the stronger upward transport of methane which converts active chlorine into HCl.

Thus, stronger vertical exchanges (large eddy diffusion coefficients) enhance the contribution of  $\text{NO}_x$  and simultaneously reduce that of  $\text{Cl}_x$  to the total ozone loss rate. In other words, the sensitivity of ozone to the CFCs decreases as the adopted eddy diffusion coefficient increases. For example, if the depletion of the ozone column for a CFC perturbation is estimated to be 7.9% for the nominal K profile (labelled 1 in Figure 2) used in this work, it is reduced to 5.9% when the larger eddy diffusion coefficient (labelled 2 in Figure 2) is adopted. Also, the non-linear regime of the  $\text{O}_3/\text{Cl}_x$  effect is reached sooner for the slower vertical exchanges as, in this case, the value of the  $\text{Cl}_x$  mixing ratio reaches that of  $\text{NO}_x$  more rapidly.

Another limitation in the accuracy of the model arises from its dimensionality. Multidimensional approaches clearly tend to represent more realistically the behavior of the atmosphere. Serious problems however remain in the representation by these models of the zonally averaged circulation and consequently of the meridional transport of trace gases such as  $\text{NO}_y$  or  $\text{Cl}_x$ .

Two-dimensional studies assuming fast horizontal diffusion (e.g., Brasseur and Bertin, 1978; U. Schmailzl, as quoted by WMO/NASA, 1986) indicate very little latitudinal and seasonal variability of the ozone response to increasing



trace gases concentration. In contrast, other models with slower eddy diffusion (e.g., Haigh and Pyle, 1982; Solomon et al., 1985; Stordal and Isaksen, 1986) suggest that transport effects will likely lead to latitudinal and seasonal variations in the ozone response. Meridional transport by planetary wave transience and dissipation remains difficult to treat accurately in 2-D models, especially for periods during which large dynamical disturbances are observed. As noted recently by Kouker and Brasseur (1986), during such events, transport becomes particularly strong and 2-D models are no longer appropriate to simulate the transport of trace species in the stratosphere, especially at high latitude.

## 5. SUMMARY

Calculations using an interactive chemical-radiative-transport one-dimensional model show that increasing concentrations in the atmosphere of source gases such as  $\text{CO}_2$ ,  $\text{CH}_4$ ,  $\text{N}_2\text{O}$  and the chlorocarbons should significantly modify the ozone and temperature distributions in the stratosphere and the troposphere.

1. Calculations based on time-dependent scenarios and assuming a 3%/yr growth for the F-11 and F-12 production with a capacity cap of 1.5 the 1984 production level, indicate that the reduction in the ozone column in the period 1940-2100 is less than 10%, assuming that the concentration of all other precursor gases remains unchanged. If, however, the concentrations of these latter gases are increasing according to the scenarios adopted in this study, the max-

imum ozone depletion is 2.8% and occurs in year 2060. The slow recovery predicted afterwards results essentially from increasing concentrations of ozone in the troposphere (due to enhanced CH<sub>4</sub> amounts). If, in addition, a 6% increase is assumed for F-113 (with an emission rate expressed in mass units which never exceeds that of F-11), the maximum ozone depletion (appearing in year 2070) is 4.2%. If a capacity cap of 2.0 times the 1984 production level is adopted for F-11 and F-12, instead of 1.5, the ozone reduction is enhanced by about 1% in the second half of the 21st century. Finally, if no capacity cap is applied, the ozone depletion calculated for a 3%/yr growth rate in the production of F-11 and F-12 becomes significantly larger than 10% after year 2050, even if a ban is imposed for the use of CFCs as propellant agents in aerosol cans. In this case the ozone response is delayed by a few years.

2. Even if the changes in the ozone column remain limited, large variations in the local concentration of O<sub>3</sub> appear in certain altitude ranges. For example, in the upper stratosphere near 40 km, reductions of 60 to 70% in the ozone concentration are predicted. These large numbers have a small influence on the ozone column since (1) at these heights, the ozone density represents less than 10% of the density near 20-25 km and (2) the reduction in the upper stratosphere is partly balanced by an ozone increase at lower levels. However these large local changes have potential effects on dynamical parameters. These effects need to be investigated by multi-dimensional models such as general circulation models (GCM).

3. Despite numerous improvements in our understanding of atmospheric chemistry in the last decade or so, large uncertainties (a factor 2-3) are associated with calculated variations in the ozone column. The largest errors are undoubtedly due to uncertainties in future emission rates, which have to be obtained from economic analyses. Errors in the calculation of the atmospheric response to specified perturbations arise not only because of uncertainties in measured rate constants or absorption cross sections, or eventual missing chemistry in the model, but also because of a lack of knowledge in the budget of active nitrogen, of approximations made in the treatment of radiative transfer and of simplified treatment of atmospheric transport. In fact, two-dimensional models (Isaksen and Stordal, 1986) should provide some insight as to the latitudinal and seasonal dependences of the ozone and temperature response to man-made perturbations.

4. The calculated ozone and temperature changes calculated by the model are believed to represent upper limits (assuming that no major reaction is missing in the chemical scheme) since (1) the amount of odd nitrogen (17-18 ppbv at 35 km) derived by the model (and by most other models) appears to be lower than the value inferred from the observation of NO, NO<sub>2</sub> and HNO<sub>3</sub>; (2) the ozone depletion obtained when using radiative code C1 (as in most simulations presented in this paper) are significantly higher than when code C2 is used; (3) the change in the ozone column predicted, as in most of this study, with weak vertical exchanges (profile 1 of the eddy diffusion coefficient -- see Fig. 2) is

larger than when eddy diffusion is assumed to be faster (profile 2); (4) the effect of the oceans which delays the temperature response of the atmosphere is not included; (5) the sources of active nitrogen in the troposphere remain constant, despite the fact that the strength of the  $\text{NO}_x$  pollution (combustion processes) is expected to grow in the future.

In conclusion, the ozone concentration and the temperature are expected to decrease in the upper stratosphere, as a result essentially of emissions of chlorofluorocarbons in the atmosphere. The ozone content is expected to increase in the troposphere, as a consequence of increasing concentrations of methane and nitrogen oxides. Due to enhanced greenhouse effects, the earth's surface should warm up by several degrees. The amplitude and even the sign of future changes in the ozone column are difficult to predict as they are strongly scenario-dependent (see also De Rudder and Brasseur, 1984). An early detection system to prevent noticeable ozone changes as a result of increasing concentrations of source gases should thus be based on a continuous monitoring of the ozone amount in the upper stratosphere rather than on measurements of the ozone column only. Measurements of  $\text{NO}_x$ ,  $\text{Cl}_x$  and  $\text{HO}_x$  will also be required for unambiguous trend detection and interpretation.

#### ACKNOWLEDGMENTS

The authors would like to thank P. J. Crutzen and C. Brühl for kindly providing them with one of the radiative codes (C1) used in the present study.

They also thank J. J. Morcrette for making available to them a copy of his radiative code (C2).

Helpful discussions with C. Brühl, R. J. Cicerone, P. J. Crutzen, R. E. Dickinson, J. C. Gille, W. Kellogg, J. T. Kiehl, F. Stordal and C. Tricot are gratefully acknowledged. This work was partly supported by the Commission of the European Communities under contract 85-B6602-11-010-11-N and by the National Aeronautics and Space Administration under contract W.-16215. G. B. is partly supported by the Belgian National Fund for Scientific Research. The National Center for Atmospheric Research is sponsored by the National Science Foundation.

## REFERENCES

- Ackerman, M., D. Frimout, C. Muller and D. J. Wuebbles, Stratospheric methane measurements and predictions, *Pure Appl. Geophys.*, *117*, 367-380, 1978.
- Blake, D. R., W. E. Mayer, S. C. Tyler, Y. Makide, D. C. Montague and F. S. Rowland, Global increase in atmospheric methane concentrations between 1978 and 1980, *Geophys. Res. Lett.*, *9*, 477-480, 1982.
- Brasseur, G., Ozone and temperature trends due to the injection of trace species in the atmosphere, in *Stratosphere*, Proceedings of a working party meeting, Commission of the European Communities, Brussels, Belgium, pp. 95- , 1984.
- Brasseur, G. and M. Bertin, The action of chlorine on the ozone layer as given by a zonally averaged two-dimensional model, *Pure Appl. Geophys.*, *117*, 436-450, 1978.
- Brasseur, G. and P. C. Simon, Stratospheric chemical and thermal response to long-term variability in solar UV irradiance, *J. Geophys. Res.*, *86*, 7343-7362, 1981.
- Brasseur, G., A. De Rudder and C. Tricot, Stratospheric response to chemical perturbations, *J. Atm. Chem.*, *3*, 261-288, 1985.
- Brasseur, G., A. De Rudder, G. M. Keating and M. C. Pitts, Response of middle atmosphere to short-term solar ultraviolet variations: 2. Theory, *J. Geo-*

*phys. Res.*, 1986.

Bruehl, C., Ph.D. Thesis, University of Mainz, Federal Republic of Germany, 1986.

Bruehl, C. H. and P. J. Crutzen, A radiative-convective model to study the sensitivity of climate and chemical composition of a variety of human activities, in *Stratosphere*, Proceedings of a working party meeting, Commission of the European Communities, Brussels, Belgium, pp. 85-94, 1984.

Burrows, J. P., T. J. Wallington and R. P. Wayne, Kinetics of the reaction of OH with ClO, *J. Chem. Soc. Faraday Trans.*, 80, 957-971, 1984.

Callis, L. B., M. Natarajan and R. E. Bougher, On the relationship between the greenhouse effect, atmospheric photochemistry, and species distributions, *J. Geophys. Res.*, 88, 1401-1426, 1983.

Callis, L. B., M. Natarajan and J. M. Russell III, Estimates of the stratospheric distributions of odd nitrogen from the LIMS data, *Geophys. Res. Lett.*, 12, 259-262, 1985.

Chemical Manufacturers Association, Production sales and calculated release of chlorofluorocarbons 11 and 12 through 1984, Report of the Fluorocarbon Program Panel, Washington, DC, October 1985.

Cicerone, R. J., D. H. Stedman and R. S. Stolarski, Estimate of late 1974 stratospheric concentration of gaseous chlorine compounds, *Geophys. Res. Lett.*, 2, 219-222, 1975.

- Connell, P. S., A parameterized numerical fit to total column ozone changes calculated by the LLNL 1-D model of the troposphere and stratosphere, Preprint, 1986.
- Connell, P. S. and D. J. Wuebbles, Ozone perturbations in the LLNL one-dimensional model -- Calculated effects of projected trends in CFC's, CH<sub>4</sub>, CO<sub>2</sub>, N<sub>2</sub>O and halons over 90 years, UCRL, 1986.
- Conseil Europeen des Federations de l'Industrie chimique (CEFIC) -- European Council of Manufacturers Federations, Halocarbon Trend Study 1983-1995, Brussels, Belgium, 1985.
- Crutzen, P. J., The influence of nitrogen oxides on the atmospheric ozone content, *Quart. J. Roy. Met. Soc.*, 96, 320-325, 1970.
- Crutzen, P. J., Ozone production rates in an oxygen, hydrogen, nitrogen oxide atmosphere, *J. Geophys. Res.*, 76, 7311-7327, 1971.
- Crutzen, P. J., Photochemical reactions initiated by and influencing ozone in unpolluted tropospheric air, *Tellus*, 26, 47-57, 1974.
- Crutzen, P. J., The role of the tropics in atmospheric chemistry, in *Geophysiology of Amazonia*, edited by R. Dickinson, Wiley Press, New York, 1986.
- Crutzen, P. J., L. E. Heidt, J. P. Krasnec, W. H. Pollock and W. Seiler, Biomass burning as a source of atmospheric gases CO, H<sub>2</sub>, N<sub>2</sub>O, NO, CH<sub>3</sub>Cl and COS, *Nature*, 282, 253-256, 1979.



- De More, W. B., D. M. Golden, R. F. Hampson, M. J. Kurylo, C. J. Howard, J. J. Margitan, M. J. Molina and A. R. Ravishankara, Chemical kinetics and photochemical data for use in stratospheric modeling, Evaluation Number 7, JPL Publication 85-37, Jet Propulsion Laboratory, Pasadena, CA, 1985.
- De Rudder, A. and G. Brasseur, Ozone in the 21st century: Increase or decrease?, in *Atmospheric ozone*, Proceedings of the Quadrennial Ozone Symposium held in Halkidiki, Greece, 3-7 September, 1984 (C. S. Zerefos and A. Ghazi, eds.), pp. 92-96, Reidel Publ. Co., Dordrecht, The Netherlands, 1985.
- Dickinson, R. E., Convergence rate and stability of ocean-atmosphere coupling schemes with a zero-dimensional climate model, *J. Atmos. Sci.*, **38**, 2112-2120, 1981.
- Dickinson, R. E. and R. J. Cicerone, Future global warming from atmospheric trace gases, *Nature*, **319**, 109-115, 1986.
- Donner, L. and V. Ramanathan, Methane and nitrous oxide: Their effects on the terrestrial climate, *J. Atmos. Sci.*, **37**, 119-124, 1980.
- Edmonds, J. A., J. Reilly, J. R. Trabalka and D. E. Reiche, An analysis of possible future atmospheric retention of fossil fuel CO<sub>2</sub>, U. S. Department of Energy, Carbon dioxide research division, Technical Report, 1984.
- Fabian, P., Halogenated hydrocarbons in the atmosphere, in *The Handbook of Environmental Chemistry, Vol. 4*, Springer Verlag, Heidelberg, pp. 23-51,

1986.

Gille, J. C. and L. V. Lyjak, Radiative heating and cooling rates in the middle atmosphere, *J. Atmos. Sci.*, in press, 1986.

Gille, J. C., J. M. Russell III, P. L. Bailey, E. E. Remsberg, L. L. Gordley, W.F.J. Evans, H. Fischer, B. W. Gandrud, A. Girard, J. E. Harries and S. A. Beck, Accuracy and precision of the nitric acid concentrations determined by the limb infrared monitor of the stratosphere experiment on Nimbus 7, *J. Geophys. Res.*, *89*, 5179-5190, 1984.

Graedel, T. E., The kinetic photochemistry of the marine atmosphere, *J. Geophys. Res.*, *84*, 273-286, 1979.

Haigh, J. D. and J. Pyle, Ozone perturbations in a two-dimensional circulation model, *Q. J. Roy. Met. Soc.*, *108*, 551-574, 1982.

Harper, D. B., Halomethane from halide ion--a highly efficient fungal conversion of environmental significance, *Nature*, *315*, 55-57, 1985.

Herman, J. R. and J. E. Mentall, O<sub>2</sub> absorption cross sections (187-225 nm) from stratospheric solar flux measurements, *J. Geophys. Res.*, *87*, 8967-8975, 1982.

Holton, J. R., A dynamically based transport parameterization for one-dimensional photochemical models of the stratosphere, *J. Geophys. Res.*, *91*, 2681-2686, 1986.

- Isaksen, I.S.A. and F. Stordal, Ozone perturbations by enhanced levels of CFCs,  $N_2O$  and  $CH_4$ : A two-dimensional diabatic circulation study including uncertainty estimates, *J. Geophys. Res.*, *91*, 5249-5263, 1986.
- Jones, R. L. and J. A. Pyle, Observations of  $CH_4$  and  $N_2O$  by the Nimbus 7 SAMS: A comparison with in-situ data and two-dimensional numerical model calculations, *J. Geophys. Res.*, *89*, 5263-5279, 1984.
- Kagann, R. H., J. W. Elkins and R. L. Sams, Absolute band strengths of halo-carbons F-11 and F-12 in the 8 to 16  $\mu m$  region, *J. Geophys. Res.*, *88*, 1427-1432, 1983.
- Keating, G. M., M. C. Pitts, G. Brasseur and A. De Rudder, Response of middle atmosphere to short-term solar ultraviolet variations: 1. Observations, *J. Geophys. Res.*, 1986.
- Keeling, C. D., The global carbon cycle: What we know and could know from atmospheric, biospheric and oceanic observations, in Proceedings of the carbon dioxide research conference: *Carbon dioxide, science and consensus*, Berkeley Springs, WV, September 19-23, 1982, U.S. Dept. of Energy publication CONF-820970, II.3-II.62, 1983.
- Khalil, M.A.K. and R. A. Rasmussen, Increase and seasonal cycles of nitrous oxide in the earth's atmosphere, *Tellus*, *35B*, 161-169, 1983.
- Kiehl, J. T. and V. Ramanathan,  $CO_2$  radiative parameterization used in climate models: Comparison with narrow band models and with laboratory

- data, *J. Geophys. Res.*, *88*, 5191-5202, 1983.
- Kiehl, J. T., C. Bruehl and T. Yamamouchi, A parameterization for the absorption due to the near infrared bands of CO<sub>2</sub>, *Tellus*, *37B*, 189-196, 1985.
- Ko, M.K.W., M. B. McElroy, D. K. Weisenstein and N. D. Sze, Lightning: A possible source of stratospheric odd nitrogen, *J. Geophys. Res.*, *91*, 5395-5404, 1986.
- Kockarts, G., Absorption and photodissociation in the Schumann-Runge bands of molecular oxygen in the terrestrial atmosphere, *Planet. Space Sci.*, *24*, 589-604, 1976.
- Kouker, W. and G. Brasseur, Transport of atmospheric tracers by planetary waves during a stratospheric warming event: A three-dimensional model simulation, *J. Geophys. Res.*, in press, 1986.
- Lacis, A., J. Hansen, P. Lee, T. Mitchell and S. Lebedeff, Greenhouse effects of trace gases, 1970-1980, *Geophys. Res. Lett.*, *8*, 1035-1038, 1981.
- Liou, K.-N. and S.-C. S. Ou, Theory of equilibrium temperatures in radiative-turbulent atmospheres, *J. Atmos. Sci.*, *40*, 214-229, 1983.
- Logan, J. A., M. J. Prather, S. C. Wofsy and M. B. McElroy, Tropospheric chemistry: A global perspective, *J. Geophys. Res.*, *86*, 7210-7254, 1981.
- Manabe, S. and R. T. Wetherald, Thermal equilibrium of the atmosphere with a given distribution of relative humidity, *J. Atmos. Sci.*, *24*, 241-259, 1967.

McClatchey, R. A., W. S. Benedict, S. A. Clough, D. E. Burch, R. F. Calfee, K.

Fox, L. S. Rothman and J. S. Garing, AFCRL atmospheric absorption line parameters compilation, Air Force Cambridge Research Laboratory Report, TR 0096, 1973.

Nicolet, M., Aeronomic reactions of hydrogen and ozone, in *Mesospheric Models and Related Experiments*, (G. Fiocco, ed.), pp. 1-51, D. Reidel Publishing Company, Dordrecht, The Netherlands, 1971.

Nicolet, M., Photodissociation of nitric oxide in the mesosphere and stratosphere: Simplified numerical relations for atmospheric model calculation, *Geophys. Res. Lett.*, 6, 866-869, 1979.

Nordhaus, W. D. and G. W. Yohe, Future carbon dioxide emissions from fossil fuels, 87-153, in *Changing climate: Report of the carbon dioxide Assessment Committee*, National Academy Press, Washington, D.C., 1983.

Owens, A. J., C. H. Hales, D. L. Filken, C. Miller, J. M. Steed and J. P. Jesson, A coupled one-dimensional radiative convective, chemistry--transport model of the atmosphere. 1. Model structure and steady state perturbation calculations, *J. Geophys. Res.*, 90, 2283-2311, 1985.

Prinn, R. G., R. A. Rasmussen, P. G. Simmonds, F. N. Alyea, D. M. Cunnold, B. C. Lane, C. A. Cardelino and A. J. Crawford, The atmospheric lifetime experiments, 5, Results for  $\text{CH}_3\text{CCl}_3$  based on three years of data, *J. Geophys. Res.*, 88, 8415-8426, 1983.

Quinn, T. H., K. A. Wolf, W. E. Mooz, J. K. Hammitt, T. W. Chesnutt and S. Sarms, Projected use, emissions, and banks of potential ozone--depleting substances, Rand Corporation, N-2282 EPA, Santa Monica, CA.

Ramanathan, V., Radiative transfer within the earth's troposphere and stratosphere, A simplified radiative-convective model, *J. Atmos. Sci.*, *33*, 1330-1346, 1976.

Ramanathan, V. and R. E. Dickinson, The role of stratospheric ozone in the zonal and seasonal radiative energy balance in the earth--troposphere system, *J. Atmos. Sci.*, *36*, 1084-1104, 1979.

Ramanathan, V., R. J. Cicerone, H. B. Singh and J. T. Kiehl, Trace gas trends and their potential role in climate change, *J. Geophys. Res.*, *90*, 5547-5566, 1985.

Ramanathan, V., L. Callis, R. Cess, J. Hansen, I. Isaksen, W. Kuhn, A. Lacis, F. Luther, J. Mahlman, R. Reck and M. Schlesinger, Climate-chemical interactions and effects of changing atmospheric trace gases, submitted to *Reviews of Geophysics*, 1986.

Rasmussen, R. A. and M.A.K. Khalil, Global atmospheric distribution and trend of methylchloroform ( $\text{CH}_3\text{CCl}_3$ ), *Geophys. Res. Lett.*, *8*, 1005-1007, 1981a.

Rasmussen, R. A. and M.A.K. Khalil, Atmospheric methane ( $\text{CH}_4$ ); trends and seasonal cycles, *J. Geophys. Res.*, *86*, 9826-9832, 1981b.

- Rasmussen, R. A. and M.A.K. Khalil, Atmospheric trace gases: Trends and distributions over the last decade, *Science*, *233*, 1623-1624, 1986.
- Roberts, R. E., J. E. Selby and L. M. Biberman, Infrared continuum absorption by atmospheric water vapor in the 8-12  $\mu\text{m}$  window, *Appl. Opt.*, *9*, 2085, 1976.
- Rogers, C. D. and C. D. Walshaw, The computation of infrared cooling rate in planetary atmospheres, *Quart. J. Roy. Met. Soc.*, *92*, 67-92, 1966.
- Russell III, J. M., J. C. Gille, E. E. Remsberg, L. L. Gordley, P. L. Bailey, S. R. Drayson, H. Fischer, A. Girard, J. E. Harries, and W.F.J. Evans, Validation of nitrogen dioxide results measured by the Limb Infrared Monitor of the Stratosphere (LIMS) experiment on Nimbus 7, *J. Geophys. Res.*, *89*, 5099-5107, 1984.
- Schlesinger, M. E., A review of climate model simulation of CO<sub>2</sub> induced climatic change (Report No 41), Climatic Research Institute, Oregon State University, Corvallis, Oregon, 1983.
- Schoeberl, M. R. and D. F. Strobel, The zonally averaged circulation of the middle atmosphere, *J. Atmos. Sci.*, *35*, 577-591, 1978.
- Simmonds, P. G., F. N. Alyea, C. A. Cardelino, A. J. Crawford, D. M. Cannold, B. C. Lane, J. E. Lovelock, R. G. Prinn and R. A. Rasmussen, The atmospheric lifetime experiment, 6, Results from carbon tetrachloride based on 3 years data, *J. Geophys. Res.*, *88*, 8427-8441, 1983.

- Singh, H. B., L. J. Salas, H. Shigeishi and E. Scibner, Atmospheric halocarbons, hydrocarbons, and sulfur hexafluoride, global distributions, source and sinks, *Science*, *203*, 899-903, 1979.
- Solomon, S., R. R. Garcia and F. Stordal, Transport processes and ozone perturbations, *J. Geophys. Res.*, *90*, 12981-12989, 1985.
- Stolarski, R. S. and R. J. Cicerone, Stratospheric chlorine: A possible sink for ozone, *Can. J. Chem.*, *52*, 1610-1615, 1974.
- Stordal, F., I.S.A. Isaksen and K. Horntveth, A diabatic circulation two-dimensional model with photochemistry: Simulations of ozone and long-lived tracers with surface sources, *J. Geophys. Res.*, *90*, 5757-5776, 1985.
- Stordal, F. and I.S.A. Isaksen, Ozone perturbations due to increases in  $N_2O$ ,  $CH_4$  and chlorocarbons: two-dimensional time-dependent calculations, submitted to *Tellus*, 1986.
- Thompson, A. M. and R. J. Cicerone, Atmospheric  $CH_4$ , CO and OH from 1860 to 1985, *Nature*, *321*, 148-150, 1986.
- Tricot, C. and A. Berger, Modelling the response of temperature to changes in trace gases: a review with emphasis on the transient response, submitted to *Climate Dynamics*, 1986.
- U.S. Standard Atmosphere, NOAA-S/T 76-1562, Supt. of Documents, U.S. Government Printing Office, Washington, DC, 1976.



- Wang, W.-C. and G. Molnar, A model study of the greenhouse effects due to increasing atmospheric  $\text{CH}_4$ ,  $\text{N}_2\text{O}$ ,  $\text{CF}_2\text{Cl}_2$  and  $\text{CFCl}_3$ , *J. Geophys. Res.*, **90**, 12971-12980, 1985.
- Wang, W.-C., Y. L. Yung, A. A. Lacis, T. Mo and J. E. Hansen, Greenhouse effect due to man-made perturbation of trace gases, *Science*, **194**, 685-690, 1976.
- Wang, W.-C., D. J. Wuebbles, W. M. Washington, R. G. Isaacs and G. Molnar, Trace gases and other potential perturbations to global climate, *Rev. of Geophysics*, **24**, 110-140, 1986.
- Weiss, R. F., The temporal and spatial distribution of tropospheric nitrous oxide, *J. Geophys. Res.*, **86**, 7185-7195, 1981.
- World Meteorological Organization (WMO) and National Aeronautics and Space Administration (NASA), Atmospheric Ozone 1985. Assessment of our understanding of the processes controlling its present distribution and change, 1986.
- Wuebbles, D. J., Chlorocarbon emission scenarios: potential impact on stratospheric ozone, *J. Geophys. Res.*, **88**, 1433-1443, 1983.
- Wuebbles, D. J., F. M. Luther and J. E. Penner, Effect of coupled anthropogenic perturbations on stratospheric ozone, *J. Geophys. Res.*, **88**, 1444-1456, 1983.
- Wuebbles, D. J., M. C. McCracken and F. M. Luther, A proposed reference set of scenarios for radiatively active atmospheric constituents, U.S. Depart-

ment of Energy, DOE/NBB-066, 1984.

Yamanouchi, T., Experimental study on the absorption properties of the near infrared atmospheric bands (in Japanese), Ph.D. thesis, Tohoku University, 287 pp., 1977.

Yung, Y. L., M. B. McElroy and S. C. Wofsy, Atmospheric halocarbons: a discussion with emphasis on chloroform, *Geophys. Res. Lett.*, 2, 397-399, 1975.